NAVAL AIR WARFARE CENTER AIRCRAFT DIVISION
PATUXENT RIVER, MARYLAND

TECHNICAL INFORMATION MEMORANDUM

REPORT NO: NAWCADPAX/TIM-2016/191

CFD ANALYSIS OF A MANEUVERING F/A-18E SUPER HORNET

by

Bradford E. Green
David B. Findlay

12 October 2016

Approved for public release.

DEPARTMENT OF THE NAVY
NAVAL AIR WARFARE CENTER AIRCRAFT DIVISION
PATUXENT RIVER, MARYLAND

NAWCADPAX/TIM-2016/191
12 October 2016

CFD ANALYSIS OF A MANEUVERING F/A-18E SUPER HORNET

by

Bradford E. Green
David B. Findlay

RELEASED BY:

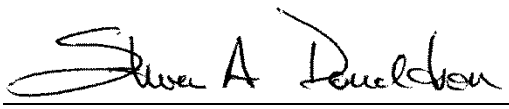

12 Oct 2016

STEVEN DONALDSON / AIR-4.3.2 / DATE
Head, Aeromechanics Engineering Division
Naval Air Warfare Center Aircraft Division

REPORT DOCUMENTATION PAGE

Form Approved
OMB No. 0704-0188

1. REPORT DATE	2. REPORT TYPE	3. DATES COVERED
12 October 2016	Technical Information Memorandum	2016

4. TITLE AND SUBTITLE

CFD Analysis of a Maneuvering F/A-18E Super Hornet

5a. CONTRACT NUMBER

5b. GRANT NUMBER

5c. PROGRAM ELEMENT NUMBER

6. AUTHOR(S)

Bradford E. Green
David B. Findlay

5d. PROJECT NUMBER

5e. TASK NUMBER

5f. WORK UNIT NUMBER

7. PERFORMING ORGANIZATION NAME(S) AND ADDRESS(ES)

Naval Air Warfare Center Aircraft Division
Code 4.3.2.1
Patuxent River, MD 20670

8. PERFORMING ORGANIZATION REPORT NUMBER

NAWCADPAX/TIM-2016/191

9. SPONSORING/MONITORING AGENCY NAME(S) AND ADDRESS(ES)

Office of Naval Research
Code 35
875 N Randolph Street
Arlington, VA 22203

10. SPONSOR/MONITOR'S ACRONYM(S)

11. SPONSOR/MONITOR'S REPORT NUMBER(S)

12. DISTRIBUTION/AVAILABILITY STATEMENT

Approved for public release.

13. SUPPLEMENTARY NOTES

14. ABSTRACT

The goal of the current study was to determine if computational fluid dynamics is capable of accurately predicting the forces and moments on the F/A-18E Super Hornet while performing several complicated maneuvers. Past F/A-18E computational studies have mainly focused on static wind-tunnel scale calculations with the results being compared to existing wind-tunnel data. In recent years, some pitching calculations were conducted at wind-tunnel scale to increase the throughput of the computational results. Furthermore, recent improvements in the tools and methods allow for moving vehicles with arbitrary motions of surfaces. These enabling capabilities and successful calculations increased confidence that actual maneuvers could be evaluated at full-scale. During this study, several F/A-18E maneuvers were evaluated. The calculations for this study were conducted at full-scale and the results were compared to data from flight tests and the F/A-18E validated flight simulation database. The maneuvers evaluated during this study included a pitch/roll/yaw doublet maneuver; a pitch captures maneuver, a 1-g full-stick roll maneuver, a constant-g windup turn maneuver and a trimmed longitudinal stick doublet maneuver. In each case, the effect of the moving aircraft and the changing flaps and control surfaces were taken into account. Both deforming mesh and overset gridding approaches were used. Time-step studies were conducted to confirm the time-accuracy of the results. In addition to these maneuvers, a pitch-damping calculation was evaluated to determine the pitch-damping coefficient. Overall, the comparisons between the computational results and the truth data were favorable. However, there is still room for improvement.

15. SUBJECT TERMS
Computational Fluid Dynamics (CFD); F/A-18E; Super Hornet

16. SECURITY CLASSIFICATION OF:			17. LIMITATION OF ABSTRACT	18. NUMBER OF PAGES	19a. NAME OF RESPONSIBLE PERSON
a. REPORT	b. ABSTRACT	c. THIS PAGE			19b. TELEPHONE NUMBER (include area code)
Unclassified	Unclassified	Unclassified	SAR	60	David Findlay 342-8545

Standard Form 298 (Rev. 8-98)
Prescribed by ANSI Std. Z39-18

SUMMARY

The goal of the current study was to determine if computational fluid dynamics is capable of accurately predicting the forces and moments on the F/A-18E Super Hornet while performing several complicated maneuvers. Past F/A-18E computational studies have mainly focused on static wind-tunnel scale calculations with the results being compared to existing wind-tunnel data. In recent years, some pitching calculations were conducted at wind-tunnel scale to increase the throughput of the computational results. Furthermore, recent improvements in the tools and methods allow for moving vehicles with arbitrary motions of surfaces. These enabling capabilities and successful calculations increased confidence that actual maneuvers could be evaluated at full-scale. During this study, several F/A-18E maneuvers were evaluated. The calculations for this study were conducted at full-scale and the results were compared to data from flight tests and the F/A-18E validated flight simulation database. The maneuvers evaluated during this study included a pitch/roll/yaw doublet maneuver; a pitch captures maneuver, a 1-g full-stick roll maneuver, a constant-g windup turn maneuver and a trimmed longitudinal stick doublet maneuver. In each case, the effect of the moving aircraft and the changing flaps and control surfaces were taken into account. Both deforming mesh and overset gridding approaches were used. Time-step studies were conducted to confirm the time-accuracy of the results. In addition to these maneuvers, a pitch-damping calculation was evaluated to determine the pitch-damping coefficient. Overall, the comparisons between the computational results and the truth data were favorable. However, there is still room for improvement.

ACKNOWLEDGMENTS

The authors would like to gratefully acknowledge the Office of Naval Research (ONR) and the CREATE/AV program for providing funding for this project. In particular, special thanks goes to ONR Aircraft Technology program managers Drs. Judah Milgram and Doug Smith of Code 351 for their continued support and guidance to allow this work to prosper and continue. The authors would also like to thank the HPCMP for providing the essential compute resources for this work. In addition, the authors would like to acknowledge Dr. David McDaniel of the CREATE-AV team for his exceptional guidance during this study.

Contents

INTRODUCTION

Announced as a National Naval Responsibility in 2011, the Sea-Based Aviation (SBA) capability consists of the operation of aircraft to, from, and on various surface ship platforms (reference 1). The maritime role of naval aircraft is complex, demanding, and unique. The ability to operate to/from a ship at sea has a dominant influence on the design of the aircraft. The largest challenge involves the dynamic interface between aircraft and surface vessel, requiring a high degree of precision maneuvering to be able to safely launch from and land aboard a moving ship deck in adverse weather, wind, and waves. Additionally, air vehicles must be multi-mission capable for a diverse set of mission tasks. While the SBA capability involves a range of air vehicle types and ship classes, one of the key capabilities consists of fixed wing aircraft operations from aircraft carriers. The current study involves research of enabling technologies aimed at improved capability for a computational-based design/analysis of multi-mission capable carrier-based fixed wing aircraft.

The Office of Naval Research (ONR), in partnership with NAVAIR, as key members of the U.S. Naval Aviation Enterprise (NAE), sponsors and executes the SBA broad technology development initiative. The SBA initiative seeks innovations needed to provide key technologies, expertise, tools and methods, and advanced concepts/systems toward the abilities of aircraft to perform enhanced ship-board operations with increased performance, improved safety, reduced cost, diminished program risk, all with less development time. SBA is clearly aimed at addressing the NAE aircraft/ship integration technology objective. Within SBA there are five aeromechanics related thrust areas: (1) Virtual Dynamic Interface (VDI), (2) Rotor-Wing Advanced Handling Qualities and Control, (3) Fixed-Wing Improved Aerodynamics and Control, (4) Enhanced Fixed-Wing VSTOL Operations, and (5) Sea-based Automated Landing and Recovery Systems. The vision of the VDI thrust area is to enable high fidelity accurate, efficient and robust modeling and simulation of launch and recovery capabilities for sea-based naval aircraft, manned and unmanned, fixed wing and rotary wing, and to utilize off-line or piloted flight simulations for virtual replication of shipboard flight operations. A portion of the intent is to significantly augment the current at-sea testing-based process to establish and certify aircraft-ship interface operating envelopes. Within the VDI thrust area are a set of near, mid, and far-term goals. To achieve the goals, a detailed roadmap has been established. This roadmap contains a set of science and technology (S&T) tasks that are interlinked in order to most effectively advance the state-of-the-art. One of these specific tasks is called Dynamic Modeling of Nonlinear Databases with Computational Fluid Dynamics (DyMOND-CFD). In particular, DyMOND-CFD is aimed primarily at enabling technologies toward the problem of modeling fixed-wing aircraft during aircraft-carrier ship takeoff and landing maneuvers. The work presented in this report is an element of the recent DyMOND-CFD project.

A. Problem Statement

During critical design driver maneuvers such as carrier launch and approach, or up and away strike for that matter, depiction of the dynamic unsteady effects of rapid motions of both the vehicle and its associated control surfaces is a known technical challenge. When aircraft maneuver rapidly, or during rapid control surface motions, at low forward speeds, the impact of unsteady flow phenomena becomes more pronounced. Moreover, if the vehicle motions are affected by translations of flow separation points, variations of vortex breakdown locations, or rapid dynamics of the lifting surfaces the aerodynamics tend to be more unsteady and nonlinear

in nature. This effect is in part caused by the associated time scales of separated flow and vortex shedding being significantly longer than convective phenomena involving circulation and surface adjacent boundary layers. The objective of the DyMOND-CFD project is to develop reliable and robust computational-based processes for predicting nonlinear and unsteady aerodynamic characteristics of naval fixed-wing aircraft performing in-flight maneuvers at full scale, below and beyond stall boundaries including arbitrary vehicle maneuvering and rapid control surface deflections. Furthermore, the intent is to utilize these predictions to create improved flight simulation models for use within the VDI SBA S&T thrust area to aid developments in the direction of improved vehicle design/analysis and pilot training. The enhanced processes will include capabilities for efficiently establishing accurate databases for nominal, as well as off-nominal, conditions to include adverse flight scenarios. The intent is to include the dynamic characteristics through the most challenging situations depicted by nonlinear unsteady aerodynamic conditions.

Since one of the important disciplinary elements for development of naval sea-based aircraft is prediction of flight dynamic characteristics of the full vehicle, this is a focus of the current study. CFD offers the potential for significantly increasing the basic prediction and understanding of aircraft and flow phenomena associated with requirements for satisfactory aircraft dynamic stability, control, and associated handling characteristics. With continued interest in improving the research, development, acquisition, test and evaluation, and sustainment processes to develop and maintain a system that meets requirements within expected cost and schedule, there is a need to determine the flight dynamic characteristics from as early in the design process as possible to the later in-service engineering applications, both reliably and efficiently. The DyMOND-CFD project focuses on this need.

B. Background

Increased demand for flight dynamics and performance capabilities of modern sea-based aircraft have highlighted the deficiency of classical techniques for determination of stability, control or aeromechanic derivative-based modeling for representation of aircraft aerodynamic forces. Of particular importance is dependence on significant motion rate effects on static and dynamic derivatives. Though these effects were first studied in the 1950’s, in the past they have often been neglected due to relatively low rates and amplitudes of motions attributed to air vehicle use (reference 2). It is now accepted that improvements are needed in the modeling of nonlinear, time-dependent aerodynamic responses during maneuvers, both to increase flight characteristics and avoid unwanted responses in extreme off-nominal conditions.

The conventional stability and control (S&C) derivative-based modeling widely remains essentially a quasi-steady aerodynamic representation of the aircrafts dynamics. When motion time history becomes significant, then an unsteady aerodynamic model is necessary. As a first step, the basic assumption of small-perturbation motion is imposed, allowing for an aerodynamic retort to the aircrafts motions to be represented as a linear dynamic system. The assumption of linearity is a common one with unsteady aerodynamics, particularly when attempting aeroelastic analysis. A component of “weak” nonlinearity can be implemented through changing parameters with angle of attack (AOA) for example. Linear aerodynamic models typically fall into four basic categories: (1) time domain, (2) frequency domain, (3) Laplace domain, and (4) state-space representation. A study by Greenwell presents a useful brief overview of these forms of unsteady aerodynamics and modeling of maneuvering aircraft (reference 3). While nonlinear unsteady aerodynamic modeling techniques have been developed, these have seen little use in practical applications. The use of such methods rely on two basic issues: a) the nonlinear unsteady

aerodynamic modeling necessary and b) how accurate and efficient is the nonlinear time-dependent method being considered. The first is dependent entirely on the aircraft and maneuver of concern. The second is an area of considerable study.

Classical aerodynamic modeling for use in flight mechanics simulations is based on basic stability derivative approach. Originated over a century ago, it denotes aircraft forces and moments based on instantaneous motion parameters and a linearized relation with these parameters. Most models in use today are an extension of this approach. Nonlinearity can be introduced through S&C derivatives being functions of the aircraft state. The problem then reduces to an ability to determine the derivatives. Typically they are measured through wind tunnel testing; however, more recently investigations include CFD as a means to this end. However, it has been shown that this technique has clear challenges. Reference 3 discusses limitations of the stability derivative model for modern combat aircraft maneuvers, in particular the problem of motion frequency effects in static and dynamic derivatives from small-amplitude oscillatory wind-tunnel testing. Greater time-dependencies are represented with terms to account for lag effects and when certain terms are implemented with frequency dependency. These models in turn account for immediate past history effects. Such models are utilized with success for a majority of aircraft dynamics modeling. However, these models do not allow for strong time-dependencies and out-of-phase effects. Consequently, efforts have considered techniques to account for additional historesis effects. A rigorous series of studies by Tobak and Schiff produced successful results (references 4 and 5). The approach involved nonlinear functional representations. Although the techniques proved difficult to implement, applications did produce promising results. Another technique involves representing aerodynamics via differential equations providing a more physics-based representation. Goman and Khrabrov showed this in a generalized implementation (reference 6). To date, there is no widely accepted industry standard approach to unsteady nonlinear aerodynamic modelling. This paper attempts to add to the wider body of work in this key area of study. While the approach of the present study includes full unsteady nonlinear depictions through the use of time-dependent CFD, the study by Kyle, et.al., outlines a useful comparison of several the fundamental analytical modeling methods (e.g., nonlinear indicial response method) previously developed (reference 7)

The prediction of aerodynamic coefficients for flight configurations is essential in assessing the performance of new designs. Accurate determination of aerodynamics is critical to the low-cost development of new capabilities, system control laws, and increased operational performance. Although actual flight testing of advanced systems will undoubtedly be an essential ingredient in the eventual success of any sea-based aircraft programs, it is both expensive and time consuming. Computer simulations can and have provided an effective means to determine the unsteady aerodynamics and flight mechanics of air vehicles (references 8-13). Use of high-performance computers to model, simulate, and test alternative designs, is a proven response to this requirement. Recent advances made in high-performance computing and CFD technologies have the potential for greatly reducing the design costs while providing a more detailed understanding of the complex aerodynamic physics than the understanding achieved through sub-scale experiments and actual flight testing.

Time-accurate or unsteady CFD modeling techniques have proven more challenging but are increasingly being used for numerical prediction of both forced and naturally unsteady aerodynamics. The accurate determination of dynamic derivatives such as the pitch, yaw, and roll damping moment coefficients is critical as they influence the dynamic stability of the air vehicle and are strong influences on the capability of the vehicles control system. Dynamic

derivatives are generally difficult to obtain by experimental or theoretical means. Wind tunnel testing can be rather expensive and in general, the dynamic derivatives are difficult to obtain in a wind tunnel and require a complex physical wind tunnel model and hardware. Flight tests can also be used to determine the dynamic derivatives. However, for either means of measuring the dynamic coefficients, the accuracy is usually not as good as it is for the static aerodynamic coefficients, especially for conditions of nonlinear aerodynamics often associated with high-lift carrier launch and recovery maneuvers. In addition, the results for the tests are only strictly valid for the specific configuration tested. Numerical methods based on linear theory and semi-empirical methods are very efficient, however, they work well for only simple and conventional configurations and are not truly suitable for complex unconventional configurations or for off-nominal flight conditions. Improved computer technology and state-of-the-art numerical procedures now enable solutions to complex, 3-D problems and these techniques that rely on time-accurate CFD methods have the greatest potential for accurate numerical prediction of the unsteady aerodynamics for general configurations and a wide range of flow conditions.

The CFD-based approach relies upon research toward advancements in flight simulation that can carry complete knowledge of aircraft dynamic characteristics enabling the potential for a more accurate representation of key nonlinear unsteady and hysteresis effects. High fidelity models of the full vehicle to include full complex high-lift configurations, vehicle attitudes and rotational rates, moving surfaces, closed loop controls and turbulent ship airwake interaction are needed to provide realistic flight dynamics data for development and testing of vehicle-handling qualities and response characteristics. The ability to effectively produce accurate robust aerodynamics predictions for full configuration high-lift aerodynamics was established within an earlier study within the DyMOND-CFD project by Green and Findlay (reference 14).

C. NAVAIR Past Related Work

For the past few decades, computational capabilities have been developed and utilized at NAVAIR for computing the flight aerodynamics of various air vehicle and weapon configurations. These studies have enabled the maturation and use of CFD for characterization of basic aerodynamics, performance, and S&C of production flight vehicles. Analysis included full-flight envelope conditions including longitudinal and lateral/directional characteristics from low to high speeds. Added effects include the impact of the flight control propulsion systems on vehicle aerodynamics. Studies began with an initial technology development effort beginning in the late 1980's investigating general unsteady effects on fixed-wing air vehicle aerodynamics (references 15-17). The studies include the first attempt by NAVAIR to employ CFD for unsteady aerodynamic analysis. The modeling included a simplified wing and moving flap configuration. The outcome was a preliminary capability which enabled more complex analysis.

Subsequent studies continued through the 1990s to include more complex full-aircraft configurations at extreme flight conditions (references 18, 19, and 20). The program of study had as a key objective the deployable capability to predict severity of structural damage due to unsteady aerodynamics associated with flow separations and vortex breakdown. The numerical analysis demonstrated an ability to capture primary unsteady flow features along with valid dominant frequency content. Further analysis included the aero-elastic capability to fully couple the unsteady aerodynamics with responsive structural dynamics. This marked the first such analysis to be successfully performed at NAVAIR opening the door for follow-on studies.

During the early part of the first decade of this century, NAVAIR, through a teaming effort with NASA and academia, devoted substantial research toward the understanding and prediction of the transonic abrupt wing stall phenomenon associated with numerous strike-type combat

aircraft (references 21 and 22). The program was successful in characterizing the underlying physics causing the phenomenon as well as developing and demonstrating innovations toward the ability to analyze abrupt wing stall aerodynamics. Several CFD methods where used. Although useful information was obtained with steady-state analysis, due to the unsteady nature of the event, a time-accurate CFD with hybrid Reynolds-Averaged Navier-Stokes/Large-Eddy Simulation computational approach proved most useful.

Although CFD could be used in conjunction with wind-tunnel tests to find potential problems, the S&C engineers require further applications and calibrations of CFD for their area of expertise. CFD has been used with success to predict the aerodynamic performance of aircraft and for flow diagnostics, but CFD has not been widely used for force and moment calculations for S&C. This “gap” between the traditional uses of CFD and the needs of the S&C community led to partnerships between CFD users and the S&C community, NASA, with DoD and industry, established the Computational Methods for S&C (COMSAC) program in 2003 (reference 23). The COMSAC program was formed to focus CFD tools to applications in S&C and to improve communications between CFD and S&C specialists. Dozens of CFD experts and S&C engineers from government and industry defined their present and future needs. Stimulated by the COMSAC initiative, an Integrated Software Development Portfolio within the U.S. DoD High Performance Computing Modernization Program (HPCMP) named Collaborative Simulation and Testing (CST) and led by NAVAIR performed multi-phased research toward CFD for S&C (reference 24). In the first phase of the project, CFD was used to predict the static longitudinal and lateral/ directional S&C characteristics of the preproduction F/A-18E at two transonic Mach numbers. The results of this work are presented in their entirety in reference (reference 25). The correlation of CFD with the wind-tunnel data was generally very good. More work was required, however, to analyze differences apparently caused by effects of complex aerodynamic unsteadiness near wing stall. The agreement between the CFD results and the wind-tunnel data for the longitudinal S&C characteristics was good, although the agreement near wing stall was poor. The general character of the longitudinal control effectiveness was predicted reasonably well by CFD. For the most part, CFD did a good job of predicting the lateral/directional S&C characteristics of the aircraft at the transonic conditions. At wing stall, large differences existed between results from two wind tunnels as well as CFD. Above wing stall at Mach 0.9, the CFD results were dependent upon the initial conditions of the calculation because of the unsteady nature of the flow. Redoing the calculations with different initial conditions resulted in good agreement between wind tunnel and CFD. In the second phase of the project, CFD was used to predict the longitudinal S&C characteristics of the preproduction F/A-18E with neutral and full nose-down control at low-speed, high AOA conditions. The results of this work are presented in reference 26. Calculations were performed for low speeds and angles of attack between 0 and 60 deg. Initially, the Spalart–Allmaras (SA) turbulence model was used. The CFD results using SA correlated well with the wind tunnel data for angles of attack below 40 deg. Above 40 deg, however, CFD differed from wind tunnel data. Despite poor correlations at higher angles of attack, tail effectiveness was accurately predicted for the full range of angles of attack. Improved correlation with wind tunnel data was achieved at 60 deg using Menter’s shear stress transport turbulence model. The third and final, phase of CFD calculations performed within the CST portfolio are presented in reference 27. In this phase of the project, the goal was to assess the ability of CFD to predict the aerodynamic roll-damping characteristics of the F/A-18E Super Hornet at transonic speeds. Roll-damping characteristics can determine a number of critical lateral handling qualities, including wing drop, wing rock, and nonlinear response to control

inputs. Prediction of aerodynamic roll damping for transonic, separated-flow conditions is particularly difficult. The aerodynamic behavior of contributing factors can be highly nonlinear with rate of roll, discontinuous or time dependent, as well as other ill-behaved trends. In addition, the extraction of values of roll damping from flight data is very challenging because of large-amplitude motions, lack of repeatability in some maneuvers, and possible uncontrollable maneuvers. If CFD can augment the conventional tools used to predict roll damping, it could become a major advance in the state of the art. Before starting the computations, the CFD flow solver employed was modified to include a rolling swirl component of the velocity about the wind axis of the aircraft. With this modification, the aircraft effectively rolls at a constant rate about the wind axis and the roll-damping characteristics of the aircraft could be estimated at the expense of a steady-state CFD calculation. Although the results are compared with an aircraft that is rolling about the body axis instead of the wind axis, only low angles of attack would be considered and the difference in roll damping that result are expected to be small. The results of this study indicate that CFD can be useful for screening a configuration for potential loss of roll damping and any associated deterioration of lateral handling qualities.

At this point with the demonstrated validated success and a substantial level of confidence in process robustness, a case was built to deploy CFD for use as a primary source of aerodynamic data in a flight clearance application. Reference 28 summarizes the approach taken and the results obtained. The data involved in-flight vehicle aerodynamic forces and moments including control surface deflection and power setting effects. Efficient analysis turn-around time to support acquisition program of record was demonstrated. However, this application was limited to steady plus static derivative data allowing for only basic flight dynamics assessments.

Beginning in 2008, the DoD HPCMP began the initiative to improve DoD acquisition program timeline, cost, and performance through the use of Computational Science and Engineering (CSE) tools for aircraft, ships, and radio-frequency antenna design and analysis. The resulting program is called the Computational Research and Engineering Acquisition Tools and Environments (CREATE) program. CREATE is a 12-year development program executed by a tri-service team. The air vehicle portion of CREATE is referred to as CREATE-AV and headed by Dr. Robert Meakin of the DoD HPCMP. CREATE-AV is aimed at developing key tools sufficient for fixed-wing, rotary-wing, and propulsion integration analysis. The fixed-wing analysis tool, referred to as Kestrel, is an integrated product written in modular form with a Python infrastructure to allow growth to additional capabilities as needed (reference 29). Computational efficiency will also be improved by targeting the next generation peta-flop architectures envisioned for the 2020+ time frame. The need for Kestrel developed from the fact that existing computational resources (hardware and CSE software) are insufficient to generate decision data in a timely enough way to impact acquisition processes. Kestrel is targeted toward simulating multi-disciplinary physics such as aero-propulsion integration, fluid-structure interactions, moving control surfaces, weapon/store carriage and release, and coupled flight control systems. The Kestrel software product is to address these needs for fixed-wing aircraft in flight regimes ranging from subsonic through supersonic flight, including maneuvers, multi-aircraft configurations, and operational conditions. The NAVAIR CFD group is a primary contributor to the CREATE-AV effort. The majority of the quality assurance and version evaluation tasks are performed at NAVAIR. The NAVAIR CFD group continues to investigate utilization of Kestrel for aircraft flight dynamics analysis. A recent study by Green evaluated the ability of Kestrel to analyze S&C characteristics of the F/A-18E sea-based strike aircraft (reference 30). Results of the study showed significant progress of the Kestrel development

team. The capabilities and accuracy of results demonstrated a basic capability to predict S&C characteristics of the strike aircraft at both wind tunnel and full scale. Computations included aircraft static and dynamic conditions. Reasonable levels of fidelity in results showed success in abrupt wing stall computations. An initial step toward predicting a maneuvering aircraft was presented. Although control surfaces are fixed, the ability to pitch and yaw the aircraft in a time-dependent manner was demonstrated. The study in reference (reference 30), along with recent related studies, has led to appreciable confidence in the use of Kestrel within the DyMOND-CFD project.

This paper presents a next evolution toward the ultimate goal of accurate and efficient prediction of in-flight unsteady and nonlinear aerodynamics of a sea-based strike aircraft. The main contribution toward that end is a demonstration of direct computations of complete maneuvers of an F/A-18E. The virtual maneuvers mimic a set of typical actual flight-test maneuvers. The analysis is performed by inputting the maneuver time history through prescribed vehicle and surface motions. The following sections will first discuss the analysis methods and tools employed throughout this study. Next, the paper discusses the technique utilized to replicate the set of maneuvers. Subsequent sections present the results for each of the different maneuvers considered. The final section provides a summary of the effort and results presented.

I. Discussion of CFD Tools Used for this Study

In this section, the CFD tools that were used during this study are discussed. These tools include the grid generation tools as well as the CFD flow solvers.

A. TetrUSS Grid Generator

The Tetrahedral Unstructured Software System (TetrUSS) was used to generate surface and volume grids of the F/A-18E Super Hornet during this study (reference 31). TetrUSS was developed at NASA Langley Research Center, Hampton, VA. TetrUSS uses GridTool, VGrid, and Postgrid to generate unstructured tetrahedral grids. While viscous grids were generated during this study, it is also possible to generate inviscid grids with TetrUSS.

After a water-tight CAD geometry has been obtained, the grid generation process begins using GridTool (reference 32). In GridTool, a series of points and curves are used to form patches on the surface of the geometry. Next, sources that control the size and density of the cells in the grid are created. VGrid then uses these patches and sources to generate an unstructured tetrahedral grid on the geometry. VGrid is run three times during the grid generation process. During the first run of VGrid, a surface grid comprised of triangles is generated. After obtaining an acceptable surface grid, VGrid is run again using an advancing-layers method to generate the cells in the boundary layer (reference 33). The normal spacing at the wall and the number of layers in the viscous part of the grid are controlled by three variables that are specified within GridTool. A separate tool called usgutil is used to determine the values for these three variables. The inputs to usgutil are the Reynolds number, the desired number of viscous layers, and the desired stretching of those layers. In the final pass through VGrid, the inviscid volume grid is generated using the advancing-front method (reference 34). Postgrid is then used in the final step of the process to remove bad cells that were formed during the grid generation process. The final product is a full three-dimensional unstructured viscous tetrahedral grid. Since each of the geometries used during this project were symmetric, half-span grids were generated and mirrored to obtain a full-span geometry. The y-plus value of the first cell above the surface is approximately unity for each of the grids.

While the TetrUSS grid generation tool generates grids with tetrahedral cells, it is important to mention that some of the cells in the boundary layer of these grids were converted to prisms prior to running the Kestrel flow solver. The Blacksmith software from Cobalt Solutions was used to do this. This approach reduces the size of the grids, which reduces the memory and run-time requirements, and allows for more accurate computation of the flow in the boundary layer.

B. Kestrel Flow Solver

The Kestrel flow solver was used to analyze the grids that were generated during this study (references 35 and 36). Kestrel is being developed by the CREATE-AV team, which is funded by the HPCMP. Kestrel originated from the AVUS flow solver, which was developed at the Air Force Research Laboratory at Wright-Patterson Air Force Base, Dayton, OH. Kestrel is a second-order, cell-centered, finite-volume Navier-Stokes flow solver that is capable of analyzing grids with arbitrary cell topologies. Kestrel can be used to generate steady-state or time-accurate solutions. Kestrel is capable of using several different flux schemes, limiters, and turbulence models. During this study, the inviscid flux scheme of Gottlieb and Groth was used, as well as the BJ+ limiter. The Gauss-Seidel matrix scheme was used. The turbulence model used during this project was the Delayed Detached Eddy Simulation model coupled with the SA RANS-based model (reference 37). Kestrel is also capable of analyzing overset grids and grids undergoing rigid body motion. A deforming mesh approach is also available for surfaces like flaps and ailerons that are subject to deflections.

Kestrel versions 2 and 4 were used to generate the results during this study. The specific version of Kestrel will be mentioned in each section when the results are presented.

II. General Approach for Modeling Aircraft Maneuvers

In this section, the general approach that was used for modeling maneuvering aircraft will be discussed. It is important to note that this is the approach that was used during this work, but there are likely several ways to do these maneuvers and get similar results. The process may have to be adjusted slightly depending on the data that is available for the maneuver.

A. Input Data for the Maneuver

The input data used for the maneuvers investigated during this study came from flight-test and flight simulation data. The maneuver data files often come with hundreds of input variables. These variables are a function of time throughout the maneuver. In the data files used for this study, a typical time step was 0.025 sec. Fortunately, only a few of the input variables in the incoming maneuver data files were needed to generate the input data for Kestrel.

To convert these data files into usable input data for Kestrel, several steps were required. First of all, the motion of the aircraft was determined using the altitude, Mach number, AOA, angle of sideslip (AOSS), and the pitch, roll, and yaw angles. The altitude, Mach number, AOA, and AOSS within the incoming data files were obtained from the nose boom on the aircraft. The roll, pitch, and yaw angles within the incoming data files were obtained from the inertial navigation system of the aircraft. In general, the data from the nose boom is probably the most accurate. However, the roll, pitch, and yaw angles from the nose boom were not provided within the incoming maneuver data files.

With the provided data, the altitude was used to calculate the speed of sound. The Mach number and speed of sound were then used to calculate the velocity. Using the velocity, AOA, and AOSS, the u, v, and w components of aircraft velocity were calculated. A rotation matrix

was then generated using the roll, pitch, and yaw angles from the incoming maneuver data. This rotation matrix was then used to convert the u, v, and w components of velocity from the body-fixed reference frame into the inertial reference frame used by the Kestrel flow solver. The basis vectors from the rotation matrix were then used to form the inputs to the flow solver. The u, v, and w components of velocity were integrated to obtain the body-fixed x, y, and z positions of the center of rotation of the aircraft, which were also input into the flow solver. The moment reference center of the aircraft was used as the center of rotation. When running these maneuvers with Kestrel, the aircraft motion was completely prescribed with the input motion data files since the free-stream velocity, AOA, and AOSS within the Kestrel input file were zero. The average altitude for the maneuver was used as an input to Kestrel. The accuracy of the Kestrel input data was confirmed by running the flow solver in preflight mode and comparing the AOA, AOSS, velocity components, and pitch, roll, and yaw angles with the incoming maneuver data.

The incoming maneuver data also contained information regarding the flap and control surface deflections. These deflections were converted into the input format that is expected by Kestrel. In addition to the deflections themselves, the hinge lines for each flap and control surface were required inputs for Kestrel. Once again, a Kestrel preflight run was used to make sure that the Kestrel inputs provided the correct flap and control surface deflections during the maneuver.

Several seconds of data were added into the Kestrel input motion files ahead of the maneuver data to get the aircraft to the correct orientation and flap and control surface deflections prior to the beginning of the actual maneuver. This also helped to ensure that the maneuver started with a converged solution at the first time step. Newer versions of Kestrel allow the user to start the maneuver at the correct orientation and flap and control surface deflections without having to add several seconds of data ahead of the maneuver.

B. Smoothness of the Input Data

The data from the incoming maneuver data files were used to generate Kestrel input files as described above. However, comparisons between the Kestrel outputs and the maneuver data files showed that the Kestrel output data was not smooth. This was attributed to the fact that the incoming maneuver data was not smooth, even though it looked smooth at first glance. As a result, the Kestrel input files for the aircraft motion and flap and control surface deflections were smoothed prior to running Kestrel. The data was smoothed iteratively from the start to the end of the maneuver. Each five consecutive points were pulled out. A parabola was fit through the first, third, and fifth points in the subset. New values of the variables at the second and fourth points were then calculated using the resulting parabola. The new values of these two data points were then inserted back into the dataset. The variables were iteratively smoothed several times until a smooth curve resulted without the loss of critical maneuver details. Five smoothing iterations typically worked well. A sample plot of the AOA as a function of time before and after smoothing is shown in Figure 1.

C. Fixed-Flaps versus Moving Flaps

When modeling a maneuvering aircraft, it is important to model the moving flaps and control surfaces throughout the maneuver. After all, the aircraft is using the flaps and control surfaces to maneuver in the first place. When initially setting up the first F/A-18E maneuver several years ago, the flaps and control surfaces were “fixed”. This was a good initiation into the science of modeling maneuvering aircraft with Kestrel, but the resulting force and moment-coefficients did not agree well with the flight-test data. A comparison of the lift coefficient from Kestrel with

fixed flaps and control surfaces to the lift coefficient from the flight-test data for the same windup turn (WUT) maneuver is shown in Figure 2. Differences between Kestrel and the flight-test data are clearly visible and show the importance of properly modeling the flaps and control surfaces during the maneuver.

D. Deforming Mesh versus Overset Grids

Two different approaches were used to model the maneuvers during this project. In the first approach, a deforming-mesh approach was used. This approach was used to model the pitch/roll/yaw doublet left/right (L/R) steady attitude sideslip (SASS) maneuver, pitch captures, 1-g full-stick roll, and constant-g WUT maneuvers presented herein. In this approach, a single grid was used. Interface planes were used to allow the grid cells near the flaps and control surfaces to move, while the grid cells away from these areas are fixed. Interface planes were used on the inboard and outboard sides of the leading-edge flaps (LEFs), the inboard and outboard sides of the trailing-edge flaps (TEFs), the inboard and outboard sides of the ailerons and the top and bottom sides of the rudders. The TEFs and ailerons share the interface planes that exist between them. These interface planes give Kestrel a method for deforming the mesh near the flaps and control surfaces so that they may be moved as desired. Kestrel ensures that mass, momentum and energy are all conserved across these interface planes even though the cells on one or both sides are moving.

Interface planes work well as long as the moving surfaces are at a reasonable distance from each other. On the F/A-18E, the horizontal tail is reasonably close to the TEF. When attempts were made to model the movement of both of these surfaces with interface planes, the interface planes overlapped with one another and the deforming-mesh approach did not work. This issue was avoided during this project by fixing the horizontal tail during the maneuver and allowing the TEF to move with the interface planes. Each maneuver was run twice with two different horizontal tail deflections. The final solution was then determined by interpolating these two sets of results to the actual horizontal tail deflection that the aircraft experienced during the maneuver.

In the second approach, overset grids were used to model the moving flaps and control surfaces. The trimmed longitudinal stick doublet maneuver was modeled with this approach. In this approach, separate overset grids were generated around the aircraft, TEFs, TEF shrouds, ailerons, aileron shrouds, horizontal tails, and rudders. The shrouds are the geometric surfaces that help the flow go smoothly from the wing box to the TEF or aileron. The shrouds deflect on schedule with the TEF and aileron, but at a fraction of the deflection. Grids of the flaps and control surfaces were modeled for one side of the aircraft and then mirrored to obtain the grid for the other side. There are gaps between all of the overset grids, so they do not touch. For typical single-grid calculations, no gap is modeled between the horizontal tail and the aircraft fuselage. However, to model an overset horizontal tail, a small gap between the fuselage and horizontal tail was included. There is no gap between the LEFs and the wing box, so the LEFs were fixed for the trimmed longitudinal stick doublet maneuver and were not modeled as an overset grid. They were included within the aircraft grid. The fact that the LEFs were fixed during the trimmed longitudinal stick doublet maneuver is a good assumption, given that the LEFs do not move significantly during this maneuver.

The best approach for future maneuvering aircraft calculations would be a combination of these two approaches. The studies showed that overset grids should be used for large flap deflections when possible, like they were for the trimmed longitudinal stick doublet maneuver.

However, the relatively small deflections of the LEFs should be modeled using the deforming-mesh approach so that movements of the LEFs are included.

Figure 3 illustrates the F/A-18E geometry model utilized in this study. The configuration elements indicated by red descriptors are the elements that were modeled with relative motion capabilities. Figures 4, 5, and 6 show a set of interface planes created for the analysis. Figure 6 displays grid mesh arrangements for wing control surface interface planes. Figure 7 illustrates the change in interface plane grid meshing from before to after surface deflection. Figure 8 shows the F/A-18E geometry with the surface settings representative of the initial trimmed conditions entering the longitudinal stick doublet maneuver. Of interest are the large flap angles indicating a high-lift configuration synonymous with a landing approach arrangement. This model included overset grids to be employed for prescribed surface motion events.

E. Configuration Consistency

When modeling aircraft maneuvers such as these, it is desired that the CFD representation of the configuration match the exact configuration that was flight tested. With the complexities associated with modeling the complete F/A-18E that is nearly impossible. With nearly all of the maneuvers that were investigated during this study, there are differences between the CFD model and the aircraft that was flight tested. Some of these differences are small and would not be expected to change the forces and moments significantly. However, some of these differences are more significant and could have a large impact on the forces and moments. So when looking at the results in this paper, it is important to keep in mind that there are differences between the CFD models and the flight-test vehicles from which the true data were derived. At the very least, CFD should be capable of predicting the trends of the data. The magnitudes may vary slightly.

F. Time-step Studies

Time step studies were conducted to ensure that the results of these maneuvers are not dependent on the time step used. For each maneuver, the basic set of calculations was run using approximately 2,800 time steps. This was the number of time steps that would finish in 1 day on 1,024 cores on a Cray supercomputer. Running 2,800 time steps was fast and gave reasonable results for confirming that everything was set up properly. From that point, time step studies were conducted. The time step was reduced first by a factor of 4 and then 16 to generate additional results for determining the impact of the time step on the force and moment coefficients. The results of one such time step study are shown in Figures 9 and 10. In these figures, the force and moment-coefficients are plotted as a function of time for three different time steps. Rather than show the actual time step, the number of time steps are shown. Time step sizes will be addressed later in the discussion. So these cases would have run in one day, four days, and 16 days using 1024 cores on the Cray supercomputer. It is clear to see from the plots that 2,800 time steps are not adequate to resolve the force and moment-coefficients for this maneuver. While there are differences in the results between 11,200 and 44,800 time steps, they are generally small. Thus, using 11,200 time steps for this maneuver is assumed acceptable. Similar time step studies were conducted for all of the maneuvers, but will not be presented here for brevity. In the section for each maneuver, the time step that was used and the number of time steps required for the maneuver will be included. For each maneuver, five Newton sub-iterations were used.

III. Pitch/Roll/Yaw Doublet L/R SASS Maneuver

In this section, the results for the pitch/roll/yaw doublet L/R SASS maneuver will be presented. The general purpose for flying this maneuver is to collect parameter identification (PID) data and to evaluate control forces in steady sideslips, rolling and yawing moments in steady sideslips, side forces in steady sideslips, and dutch-roll characteristics on control release. The average Mach number of the maneuver is 0.816. The average altitude of the maneuver is approximately 34,400 ft. The force and moment-coefficients from Kestrel will be compared to flight-test data. Kestrel 2.2.2 was used for these calculations.

A. Grids and Approach

To evaluate this maneuver, two half-span grids were generated and mirrored to full span. The deforming mesh approach described above was used for this case. Interface planes allowed the movement of the LEFs, TEFs, ailerons, and rudders. The horizontal tail was fixed in each grid. In one grid, the horizontal tail deflection captured the lower bound of the actual horizontal tail deflection from the maneuver. In the second grid, the horizontal tail deflection captured the upper bound of the horizontal tail motion. The full-span grids contained 47 and 45 million cells, respectively. The grids contained mostly tets and prisms. After running each grid through the maneuver with Kestrel, the aerodynamic force and moment coefficients were interpolated to the actual horizontal tail deflection of the aircraft.

For the calculations, a time step of 0.006152 sec was used with five Newton sub-iterations. A time-step study was conducted to confirm that this time step was adequate to capture the force and moment coefficients for the entire maneuver. The maneuver lasted for approximately 69 sec and required 11,200 time steps given the specified time step. This was the longest maneuver investigated during this project. The angles of attack and sideslip, altitude, and velocity components for the maneuver are plotted in Figure 11. The port and starboard LEF, TEF, aileron, horizontal tail, and rudder deflections of the maneuver are shown in Figure 12. With a few exceptions, the motion of the control surfaces is symmetric between the port and starboard sides of the aircraft.

B. Results

In Figures 13 and 14, the force and moment coefficients from Kestrel are compared to the flight-test data for the pitch/roll/yaw doublet L/R SASS maneuver. The force and moment coefficients used for the “truth data” were computed by Boeing from the flight-test data using the 6-Degree of Freedom (DOF) equations and solving for the total forces and moments. They include all of the inertias, rates, accelerations, angles, etc. from flight. The equations were inverted to get the aerodynamic terms. The flight tests were conducted without instrumented engines, so Boeing uses a simulation engine model to remove the thrust contribution. Anything left over is considered drag. As a result, the drag term in this model is usually ignored by the Boeing S&C engineers, where this data was derived. The drag from the Boeing performance group is usually used instead, but the performance drag is not available for comparison here.

The lift, drag, axial-force, normal-force, and pitching-moment coefficients are plotted in Figure 13. The agreement between Kestrel and the flight-test data is very good. Kestrel predicts most of the trends and magnitudes of the flight-test data. The Kestrel results for the pitching-moment coefficient are more unsteady than the flight-test data. In addition, the axial-force coefficient from Kestrel does not agree well with the flight-test data at a time of 20 sec. The reasons for this are unknown and warrant further investigation.

The side-force, rolling-moment, and yawing-moment coefficients are plotted in Figure 14. The Kestrel results for these coefficients also agree very well with the flight-test data. Kestrel is even able to accurately predict the change in magnitude of the side-force coefficient at a time of 50 sec.

C. Computational Efficiency

The calculations for this maneuver were run on a Cray XE6 using 512 cores. Each calculation took approximately 9 days and used approximately 112,000 hr of CPU time.

IV. Pitch Captures Maneuver

In this section, the results for the pitch captures maneuver will be presented. The general purpose for flying this maneuver is to evaluate pilot-induced oscillation (PIO) tendencies and collect PID data. The average Mach number of the maneuver is 0.59. The average altitude of the maneuver is approximately 10,300 ft. The force and moment coefficients from Kestrel will be compared to data from the trusted aero database. Kestrel 2.2.2 was used for these calculations.

A. Grids and Approach

To evaluate this maneuver, two half-span grids were generated and mirrored to full span. The deforming mesh approach described above was also used for this maneuver. The LEFs, TEFs, ailerons, and rudders were allowed to move during the maneuver using interface planes. The horizontal tail was fixed in each grid. Once again, the lower and upper bounds of the horizontal tail motion were captured with the two grids. The full-span grids contained 47 and 43 million cells, respectively. The grids contained mostly tets and prisms. After running each grid through the maneuver with Kestrel, the force and moment-coefficients were interpolated to the actual horizontal tail deflection of the aircraft.

For the calculations, a time step of 0.00249 sec was used with five Newton sub-iterations. A time-step study was conducted to confirm that this time step was adequate to capture the force and moment coefficients for the entire maneuver. The maneuver lasted for approximately 28 sec and required 11,200 time steps given the specified time step. The AOA and AOSS, altitude and velocity components for the maneuver are plotted in Figure 15. This maneuver contains two large AOA spikes at times of 7 and 22 sec. The port and starboard LEF, TEF, aileron, horizontal tail, and rudder deflections of the maneuver are shown in Figure 16. The large AOA spikes that are present at times of 7 and 22 sec are also accompanied by large changes in all of the control surfaces. As a result of these changes in AOA and control surface deflections, the force and moment coefficients are expected to change.

B. Results

In Figures 17 and 18, the force and moment-coefficients from Kestrel are compared to the aero database for the pitch captures maneuver. The force and moment estimates from the aero database include all of the inertias, rates, accelerations, angles, etc. from flight. Flight-test data could not be used for comparison for this maneuver, since there was an issue with the throttle instrumentation during the flight test that resulted in unreasonable estimates of drag and axial force.

The lift, drag, axial-force, normal-force, and pitching-moment coefficients are plotted in Figure 17. The agreement between Kestrel and the aero database is very good for the lift, normal-force, and pitching-moment coefficients. Kestrel captures the trend of the data for the

drag and axial-force coefficients, but the magnitude of the results is displaced. Kestrel did a great job of capturing the effects of the spikes in AOA and the control surface deflections at times of 7 and 22 sec.

The side-force, rolling-moment, and yawing-moment coefficients are plotted in Figure 18. The Kestrel results for these coefficients also agree reasonably well with the trusted aero database. These coefficients are relatively small in magnitude, since this maneuver is primarily a longitudinal maneuver. Nonetheless, it is interesting to note that the Kestrel results for rolling-moment and yawing-moment coefficient are more unsteady than the results from the aero database.

C. Computational Efficiency

The calculations for this maneuver were run on a Cray XE6 using 512 cores. Each calculation took approximately 6 days and used approximately 77,000 hr of CPU time.

V. 1-g Full-Stick Roll Maneuver

In this section, the results for the 1-g full-stick roll maneuver will be presented. The general purpose for flying this maneuver is to collect PID data and evaluate roll performance, roll coupling/coordination and PIO tendencies. The average Mach number of the maneuver is 0.804. The average altitude of the maneuver is approximately 36,200 ft. The force and moment coefficients from Kestrel will be compared to flight-test data. Kestrel 2.2.2 was used for these calculations.

A. Grids and Approach

To evaluate this maneuver, three separate grids were used. The deforming mesh approach described above was used for this case. Interface planes allowed the movement of the LEFs, TEFs, ailerons, and rudders during the maneuver. The horizontal tail was fixed in each grid. In one grid, the horizontal tail deflection was the same on the port and starboard sides. In the other two grids, asymmetric deflections (neutral/positive and neutral/negative) were used in an effort to capture the changes in the horizontal tail deflections that occur during the maneuver. The full-span grids varied in size between 48 and 53 million cells. The grids contained mostly tets and prisms. After running each grid through the maneuver with Kestrel, the force and moment-coefficients were interpolated to the actual horizontal tail deflection of the aircraft.

For the calculations, a time step of 0.001067 sec was used with five Newton sub-iterations. A time-step study was conducted to confirm that this time step was adequate to capture the force and moment coefficients for the entire maneuver. The maneuver lasted for approximately 12 sec and required 11,200 time steps given the specified time step. This was one of the shortest maneuvers investigated during this project. The angles of attack and sideslip, altitude, and velocity components for the maneuver are plotted in Figure 19. The port and starboard LEF, TEF, aileron, horizontal tail, and rudder deflections of the maneuver are shown in Figure 20. The asymmetric deflections of the TEFs, ailerons, and horizontal tails are clearly evident in the plots. The LEF and rudder deflections are very symmetric.

B. Results

In Figures 21 and 22, the force and moment-coefficients from Kestrel are compared to the flight-test data for the 1-g full-stick roll maneuver. The force and moment coefficients used for the "truth data" were computed by Boeing from the flight-test data using the 6-DOF equations and solving for the total forces and moments. They include all of the inertias, rates, accelerations, angles, etc from flight. The equations were inverted to determine the aerodynamic terms. The flight tests were conducted without instrumented engines, so Boeing uses a simulation engine model to remove the thrust contribution. Anything left over is considered drag. As a result, the drag term in this model is usually ignored by the Boeing S&C engineers, where this data was derived. The drag from the Boeing performance group is usually used instead, but the performance drag is not available for comparison here.

The lift, drag, axial-force, normal-force, and pitching-moment coefficients are plotted in Figure 21. The agreement between Kestrel and the flight-test data for the lift and normal-force coefficients is very good. The trend of the data for the drag and axial-force coefficients is captured well by Kestrel, but the magnitude of the data is shifted slightly. The agreement for the pitching-moment coefficient is good, although the Kestrel results under predict the flight-test data between 7 and 9 sec. The reason for this disagreement is likely due to the approach in modeling the horizontal tail. From Figure 20, it is apparent that the horizontal tail deflections are asymmetric between 7 and 9 sec.

The side-force, rolling-moment, and yawing-moment coefficients are plotted in Figure 22. The Kestrel results for these coefficients generally agree appreciably well with the flight-test data. However, like the pitching-moment coefficient, the side-force coefficient is under predicted by Kestrel between 7 and 9 sec. This disagreement could also be due to the way that the effects of the asymmetric horizontal tails are being included.

C. Computational Efficiency

The calculations for this maneuver were run on a Cray XE6 using 512 cores. Each calculation took approximately 7 days and used approximately 91,000 hr of CPU time.

VI. Constant-g WUT Maneuver

In this section, the results for the constant-g WUT maneuver will be presented. The general purpose for flying this maneuver is to collect PID data and evaluate the maneuvering stability and g-limiter performance of the aircraft. The average Mach number of the maneuver is 0.735. The average altitude of the maneuver is approximately 2,700 ft. The force and moment coefficients from Kestrel will be compared to flight-test data. Kestrel 2.2.2 was used for these calculations.

A. Grids and Approach

To evaluate this maneuver, two half-span grids were generated and mirrored to full span. The deforming mesh approach described above was also used for this maneuver. The LEFs, TEFs, ailerons, and rudders were allowed to move during the maneuver using interface planes. The horizontal tail was fixed in each grid. Once again, the lower and upper bounds of the horizontal tail motion were captured with the two grids. Each full-span grid contained 47 million cells. The grids contained mostly tets and prisms. After running each grid through the maneuver with Kestrel, the force and moment-coefficients were interpolated to the actual horizontal tail deflection of the aircraft.

For the calculations, a time step of 0.004192 sec was used with five Newton sub-iterations. A time-step study was conducted to confirm that this time step was adequate to capture the force- and moment-coefficients for the entire maneuver. The maneuver lasted for approximately 47 sec and required 11,200 time steps given the specified time step. The angles of attack and sideslip, altitude and velocity components for the maneuver are plotted in Figure 23. The AOA increases significantly throughout the maneuver. It is interesting to note that the altitude during this maneuver was very low. WUTs are normally conducted at higher altitudes. The port and starboard LEF, TEF, aileron, horizontal tail, and rudder deflections of the maneuver are shown in Figure 24. The LEFs, TEFs, ailerons, and horizontal tails are generally symmetric during the maneuver. There is some asymmetry in the rudder during the maneuver.

B. Results

In Figures 25 and 26, the force and moment-coefficients from Kestrel are compared to the flight-test data for the constant-g WUT maneuver. The force and moment coefficients used for the "truth data" were computed by Boeing from the flight-test data using the 6-DOF equations and solving for the total forces and moments. They include all of the inertias, rates, accelerations, angles, etc. from flight. The equations were inverted to get the aerodynamic terms. The flight tests were conducted without instrumented engines, so Boeing uses a simulation engine model to remove the thrust contribution. Anything left over is considered drag. As a result, the drag term in this model is usually ignored by the Boeing S&C engineers, where this data was derived. The drag from the Boeing performance group is usually used instead, but the performance drag is not available for comparison here.

The lift, drag, axial-force, normal-force and pitching-moment coefficients are plotted in Figure 25. The lift, axial-force, and normal-force coefficients from Kestrel trend will with the data, but magnitude is displaced slightly. The drag coefficient from Kestrel generally agrees well with the flight-test data, although there is a small displacement at the beginning of the maneuver. The pitching-moment coefficient from Kestrel trends in the wrong direction from the data. These differences are significant. Various geometry changes were investigated in an effort to understand the reason behind the differences in pitching-moment coefficient, but the attempts were unsuccessful. More rigorous investigations are required to better understand these results.

The side-force, rolling-moment, and yawing-moment coefficients are plotted in Figure 26. The Kestrel results for the rolling-moment and yawing-moment coefficients generally agree well with the flight-test data, although there is a difference near the beginning of the maneuver. The Kestrel results for the side-force coefficient are off in magnitude from the flight-test data.

C. Computational Efficiency

The calculations for this maneuver were run on a Cray XE6 using 512 cores. Each calculation took approximately 7 days and used approximately 90,000 hr of CPU time.

VII. Trimmed Longitudinal Stick Doublet Maneuver

In this section, the results for the trimmed longitudinal stick doublet maneuver will be presented. This maneuver was selected because it shows the magnitudes of the fast control surface rates that are possible on the F/A-18E. The average Mach number of the maneuver is 0.2. The average altitude of the maneuver is approximately 1,240 ft. The force and moment coefficients from Kestrel will be compared to trusted sim data. Kestrel 4.0.13 was used for these calculations.

A. Grids and Approach

An overset approach was used to generate the grids for this maneuver. This approach is discussed above. The TEFs, ailerons, flap and aileron shrouds, and the horizontal tails were allowed to move during this maneuver. The LEFs and rudders were fixed during the maneuver. The grid system was comprised of 11 overset grids containing approximately 125 million cells. The grids contained mostly tets and prisms.

For the calculations, a time step of 0.00125 sec was used with five Newton sub-iterations. The maneuver lasted for 22 sec and required 17,700 time steps given the specified time step. The angles of attack and sideslip, altitude, and velocity components for the maneuver are plotted in Figure 27. The port and starboard TEF, aileron, and horizontal tail deflections of the maneuver are shown in Figure 28. The LEFs and horizontal tails are generally symmetric during the maneuver. There is some asymmetry in the ailerons during the maneuver. It is important to note that there are some abrupt changes in the TEF deflections at 15.5 sec and abrupt changes in the horizontal tail deflections at 13, 15.5, and 17 sec.

B. Results

In Figure 29, the force and moment-coefficients from Kestrel are compared to the sim data for the trimmed longitudinal stick doublet maneuver. The lift, drag, axial-force, normal-force, and pitching-moment coefficients are plotted in this figure. The Kestrel results generally trend well with the sim data. However, there are some differences in magnitude in the middle of the maneuver. These differences generally occur when the AOA is changing the most.

C. Computational Efficiency

The calculation for this maneuver was run on an SGI ICE X system. Due to available memory on the machine, 1,024 cores were requested, but the simulation was run on only half of the cores. The calculation took approximately 8 days and used approximately 202,000 hr of CPU time.

VIII. Pitch-Damping Calculation

In an effort to better understand the F/A-18E database, a pitch-damping calculation on the F/A-18E was conducted. Due to the success and accuracy of the F/A-18E maneuvering aircraft cases that were done during this project, it was anticipated that CFD could accurately predict the pitch-damping coefficient on the F/A-18E. Roll-damping calculations were done on the F/A-18E several years ago with much success, but this was the first attempt at modeling the pitch-damping coefficient. In this section, the results of the F/A-18E pitch-damping calculations are presented and discussed. Kestrel was used for these calculations and the results were compared to the pitch-damping coefficient in the sim database. Kestrel 4.1 was used for these calculations.

A. Grids and Approach

For this case, a full-span, unstructured grid with 91.7 million cells was used. The deflections of the leading-flaps, TEFs, and ailerons were 15 deg, 40 deg, and 40 deg, respectively. A neutral horizontal tail deflection was used. The gaps surrounding the flaps and ailerons were modeled. The solution was run at Mach 0.2 at sea-level standard conditions at an AOA of 8.1 deg. The calculations were run in two steps. In the first step, a static solution was evaluated and run to convergence. This solution was run at a time step of 0.003 sec with five Newton sub-iterations. Upon completion of this static case, the aircraft was pitched at a rate of 10 deg/sec nose over tail. This solution was restarted from the converged static case. A time step of 0.001 sec with five

Newton sub-iterations was used. The solution was run until the aircraft had pitched more than 360 deg. The pitching-moment coefficient was measured as the aircraft passed through the wings-level position after pitching 360 deg. The pitch-damping coefficient was then calculated using the equation

$$C_{m_q} = \frac{C_{m_{pitching}} - C_{m_{static}}}{\bar{q}_{pitching}}$$

where

$$\bar{q}_{pitching} = \frac{q_{pitching} c}{2V_\infty}$$

B. Results

The results for the static and pitching calculations are shown in Figure 30. On the left side of the figure, the pitching-moment coefficient for the static case is plotted as a function of time. It should be noted that while the aircraft is static, the flow field is computed as time-accurate and is expected at times to include noticeable natural unsteadiness. Although naturally oscillating, the solution is considered converged. The static pitching-moment coefficient was determined by averaging the results over the last few seconds of the solution. After this solution was finished, it was used as a restart for the pitching case. The aircraft was pitched at a rate of 10 deg/sec nose over tail. The pitching-moment coefficient during this run is plotted as a function of the aircraft pitch angle on the right side of Figure 10. At the point that the aircraft pitch angle passes through wings-level at 360 deg, the pitching-moment coefficient was determined and used in the equation above to calculate the pitch-damping coefficient. The resulting pitch-damping coefficient was negative and stable as one would expect. This value was determined to be within approximately 10% of the current value in the F/A-18E trusted sim database. This correlation is considered to be rather good.

C. Computational Efficiency

The calculations for this case were run on an IBM iDataPlex system using 2,048 cores. The static solution took approximately 20 hr and used 41,000 hr of CPU time. The pitching solution took approximately 35 hr and used 71,000 hr of CPU time.

IX. Summary

CFD has been used to analyze the F/A-18E Super Hornet undergoing several complex maneuvers. These maneuvers included a pitch/roll/yaw doublet maneuver, a pitch captures maneuver, a 1-g full-stick roll maneuver, a constant-g WUT maneuver and a trimmed longitudinal stick doublet maneuver. The flaps and control surfaces were allowed to move with the aircraft motion. In addition, a pitch-damping calculation on the F/A-18E was evaluated. This calculation was done with fixed flaps and control surfaces. Both deforming mesh and overset grid techniques were used during the course of this study. For each of the maneuvers, the force and moment coefficients from the calculations were compared to sim data, the aero database, or flight-test data. Time step studies were conducted to confirm that the results are not dependent on

the time step. The agreement for the force and moment coefficients between CFD and the truth data for the maneuvers is generally very good. In many cases, the computational results are able to predict both the trend and magnitude of the truth data. In other cases, the computational results capture the trend of the data, but not the magnitude.

This study represents the second phase of a three-phase computational project. The first phase of this work included modeling the F/A-18E Super Hornet at the high-lift aerodynamic conditions usually encountered during carrier landing. The calculations were conducted at low speed for a variety of flap and control surface deflections. Small, medium, and large deflections of the TEF were considered. The computational results were compared to F/A-18E sim data. In the third phase of this study, the TEF, and aileron on the F/A-18E were moved at very fast rates of motion to determine the aerodynamic response associated with these motions. The results of these calculations indicated that the forces and moments depend on the starting and ending deflection of the control surface and the rate at which the control surface was deflected. For cases when the TEF moved, the results were also dependent on the fixed position of the aileron. Similarly, when the aileron moved, the results were dependent on the fixed position of the TEF.

THIS PAGE INTENTIONALLY LEFT BLANK

REFERENCES

1. http://www.onr.navy.mil/Science-Technology/Departments/~/media/Files/35/NNR-Sea-Based-Aviation.ashx
2. Harper, P. and Flanigan, R., "The Effect of Rate Change of Angle of Attack on the Maximum Lift of a Small Model," NACA TN 2061, Mar 1950.
3. Greenwell, D., "A Review of Unsteady Aerodynamic Modeling for Flight Dynamics of Maneuvering Aircraft," AIAA-2004-5276, Aug 2004.
4. Tobak, M. and Schiff, L., "On the Formulation of the Aerodynamic Characteristics in Aircraft Dynamics," NASA TR R-456, Jan 1976.
5. Tobak, M. and Schiff, L., "Aerodynamic Math Modeling – Basic Concepts," AGARD Lecture Series on Dynamic Stability Parameters, AGARD-LS-114, NATO, 1981, pp. 1.1-1.32.
6. Goman, M and Khrabrov, A., "State-Space Representation of Aerodynamic Characteristics of an Aircraft at High Angles of Attack," J. Aircraft, Vol. 31, pp. 1109-1115, 1994.
7. Kyle, H., Lowenberg, M., Greenwell, D., "Comparative Evaluation of Unsteady Aerodynamic Modeling Approaches," AIAA-2004-5272, Aug 2004.
8. Findlay, D. and Hynes, M., "The Effective Use of CFD for Military Aircraft Stability and Control Evaluation," AIAA 2010-1036, Jan 2010.
9. Cummings, R. and A. Schütte, A., "An Integrated Computational/Experimental Approach to UCAV Stability & Control Estimation: Overview of NATO RTO AVT- 161", AIAA-2010-4392, Jun 2010.
10. Loeser, T., Vicroy, D., and Schütte, A., "SACCON Static Wind Tunnel Tests at DNW-NWB and 14´x22´ NASA LaRC", AIAA-2010-4393, Jun 2010.
11. Frink, N., "Strategy for Dynamic CFD Simulation on SACCON Configuration," AIAA Paper 2010-4559, Jun 2010.
12. Thompson, J.R., Frink, N.T., and Murphy, P.C., "Guidelines for Computing Longitudinal Dynamic Derivatives on Subsonic Transport", AIAA Paper 2010-4819, Jun 2010.
13. Murphy, P.C., Klein, V., Frink, N.T., and Vicroy, D.D., "System Identification Applied to Dynamic CFD Simulation and Wind Tunnel Data", presented at the AIAA Atmospheric Flight Mechanics Conference to be held in Portland, OR, 8-11 Aug 2011.
14. Green, B. and Findlay, D., "CFD Analysis of the F/A-18E Super Hornet during Aircraft-Carrier Landing High-Lift Aerodynamic Conditions," AIAA-2016-1768, SciTech 2016, San Diego, CA, Jan 2016.
15. Smith, B., "Dynamically Enhanced Sustained Lift Using Oscillating Leading-Edge Flaps," AIAA-92-2625.
16. Tseng, W., Tsung, F., and Sankar, L., "Numerical Simulation of dynamic Lift Enhancement Using Oscillatory Leading Edge Flaps," AIAA-93-0186, Jan 1993.
17. Bangalore, A., Tseng, W., Sankar, L. "A Multizone Navier-Stokes Analysis of Dynamic Lift Enhancement Concepts," AIAA-94-0164, Jan 1994.
18. Findlay, D., "Numerical Analysis of Vertical Tail Buffet," AIAA-97-0621, Jan 1997.
19. Findlay, D. and Guruswamy, G., "Numerical Analysis of Aircraft High Angle of Attack Unsteady Flows," AIAA-2000-1946, Jun 2000.
20. Findlay, D., "A Numerical Study of Aircraft Empennage Buffet," Ph.D. Dissertation, Georgia Institute of Technology, Jun 1999.

21. Woodson, S., Green, B., Chung, J., Grove, D., Parikh, P., Forsythe, J., "Understanding Abrupt Wing Stall with Computational Fluid Dynamics," Journal of Aircraft, Vol. 42, No. 3, p. 578.
22. Forsythe, J., and Woodson, S., "Unsteady Computations of Abrupt Wing Stall Using Detached-Eddy Simulation," Journal of Aircraft, Vol. 42, No. 3, p. 606.
23. Hall, R., Biedron, R., Ball, D., Bogue, D., Chung, J., Green, B., and Chambers, J., "Computational Methods for Stability and Control (COMSAC): The Time Has Come," AIAA 2005-6121, Aug 2005.
24. Findlay, D. and Wilkinson, C., "Collaborative Simulation and Test Utilizing High Performance Computing," AIAA 2007-6570, Aug 2007.
25. Green, B. E., and Chung, J. J., "Transonic Computational Fluid Dynamics Calculations on Preproduction F/A-18E for Stability and Control," Journal of Aircraft, Vol. 44, No. 2, 2007, pp. 420–426.
26. Green, B., "Computational Prediction of Nose-Down Control for the Pre-Production F/A-18E at High Angle of Attack, AIAA-2007-6724
27. Green, B., "Computational Prediction of Roll Damping for the F/E-18E at Transonic Speeds," Journal of Aircraft, Vol. 45., No. 4, pp. 1297-1304.
28. Shaffer, T., and Green, B., "CFD Generation of Flight Databases for UAVs for Use in the Flight Certification Process," AIAA-2010-1037, Jan 2010.
29. Morton, S., McDaniels, D., Sears, D., Tillman, B., and Tuckey, T., "Kestrel – A Fixed Wing Virtual Aircraft Product of the CREATE Program," AIAA-2009-338, Jan 2009.
30. Green, B., "Analysis of the Stability and Control Characteristics of the F/A-18E Super Hornet using Kestrel CFD Flow Solver," AIAA-2012-0715.
31. Frink, N. T., Pirzadeh, S., Parikh, P., Pandya, M. J., and Bhat, M. K., "The NASA Tetrahedral Unstructured Software System (TetrUSS)," The Aeronautical Journal, Vol. 104, No. 1040, Oct. 2000, pp. 491-499.
32. Samareh, J., "GridTool: A Surface Modeling and Grid Generation Tool," Proceedings of the Workshop on Surface Modeling, Grid Generation, and Related Issues in CFD Solutions," NASA CP-3291, 9-11 May 1995.
33. Pirzadeh, S., "Three-Dimensional Unstructured Viscous Grids by the Advancing Layers Method," AIAA Journal, Vol. 34, No. 1, Jan 1996, pp.43-49.
34. Löhner R and Parikh P. C., "Three-dimensional Grid Generation by the Advancing Front Method," Int.J.Num.Meth. Fluids 8, pp 1135-1149 (1988).
35. Morton, S. A., McDaniel, D. R., Sears, D. R., Tillman, B., and Tuckey, T. R., "Kestrel: A Fixed Wing Virtual Aircraft Product of the CREATE Program," AIAA-2009-0338, Jan 2009.
36. Morton, S., Eymann, T., McDaniel, D., Sears, D., Tillman, B., and Tuckey, T., "Rigid and Maneuvering Results with Control Surface and 6DoF Motion for Kestrel v2," AIAA-2011-1106, Jan 2011.
37. Spalart, P. R., and Allmaras, S. R., "A One-Equation Turbulence Model for Aerodynamic Flows," AIAA Paper 97-0644, Jan 1997.

NOMENCLATURE

C_A = aircraft axial-force coefficient
C_D = aircraft drag coefficient
C_L = aircraft lift coefficient
C_l = aircraft rolling-moment coefficient
C_m = aircraft pitching-moment coefficient
C_N = aircraft normal-force coefficient
C_n = aircraft yawing-moment coefficient
C_Y = aircraft side-force coefficient
c = mean aerodynamic chord (in.)
h = altitude (ft)
q = pitch rate (deg/sec, rad/sec)
Re_c = Reynolds number based on mean aerodynamic chord
u = x-component of velocity (in./sec)
V = velocity magnitude (in./sec)
v = y-component of velocity (in./sec)
w = z-component of velocity (in./sec)
α = angle of attack (deg)
β = angle of sideslip (deg)
δ_a = aileron deflection angle (deg)
δ_f = trailing-edge flap deflection angle (deg)
δ_l = leading-edge flap deflection angle (deg)
δ_r = rudder deflection angle (deg)
δ_s = horizontal tail deflection angle (deg)
$\theta_{a/c}$ = pitch angle of aircraft (deg)

THIS PAGE INTENTIONALLY LEFT BLANK

FIGURES

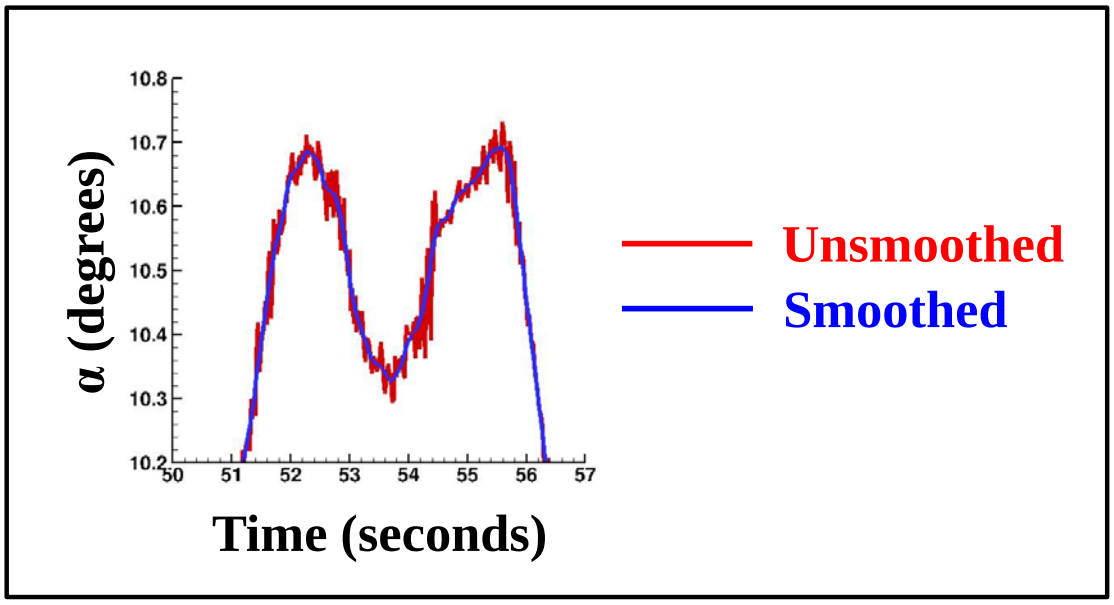

Figure 1: Effect of Smoothing on the Input Maneuver Data

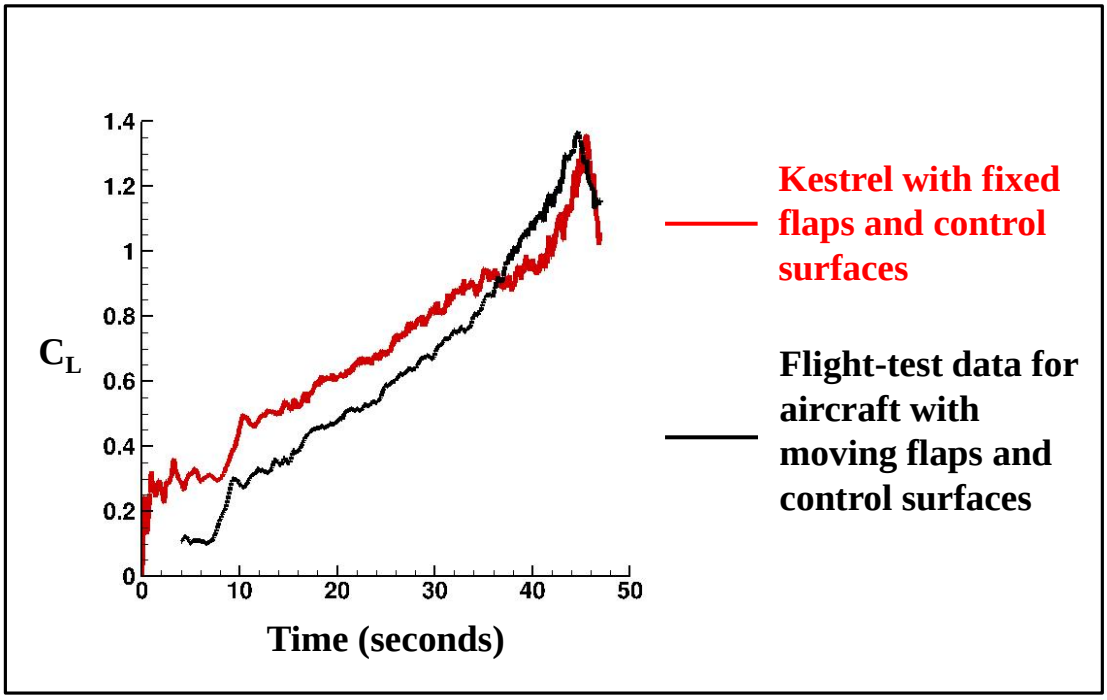

Figure 2: Importance of Modeling Moving Flaps and Control Surfaces during a Maneuver

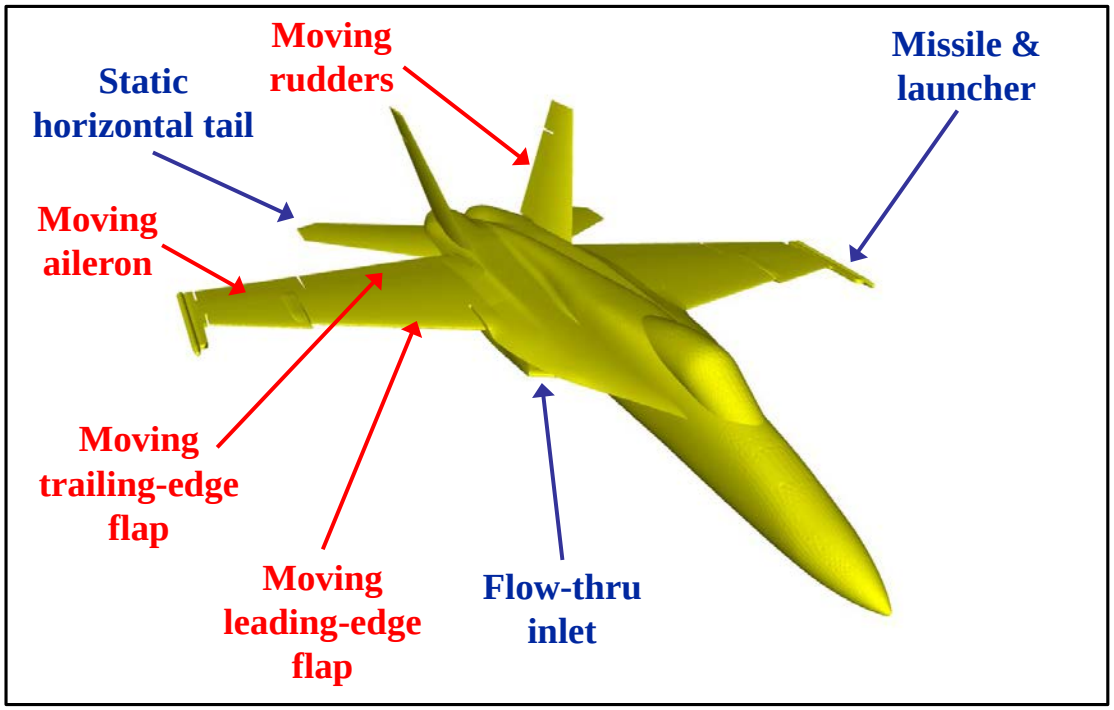

Figure 3: Basic F/A-18E Geometry Used for the Pitch/Roll/Yaw Doublet L/R SASS, Pitch Captures, 1-g Full-Stick Roll, and Constant-g WUT Maneuvers

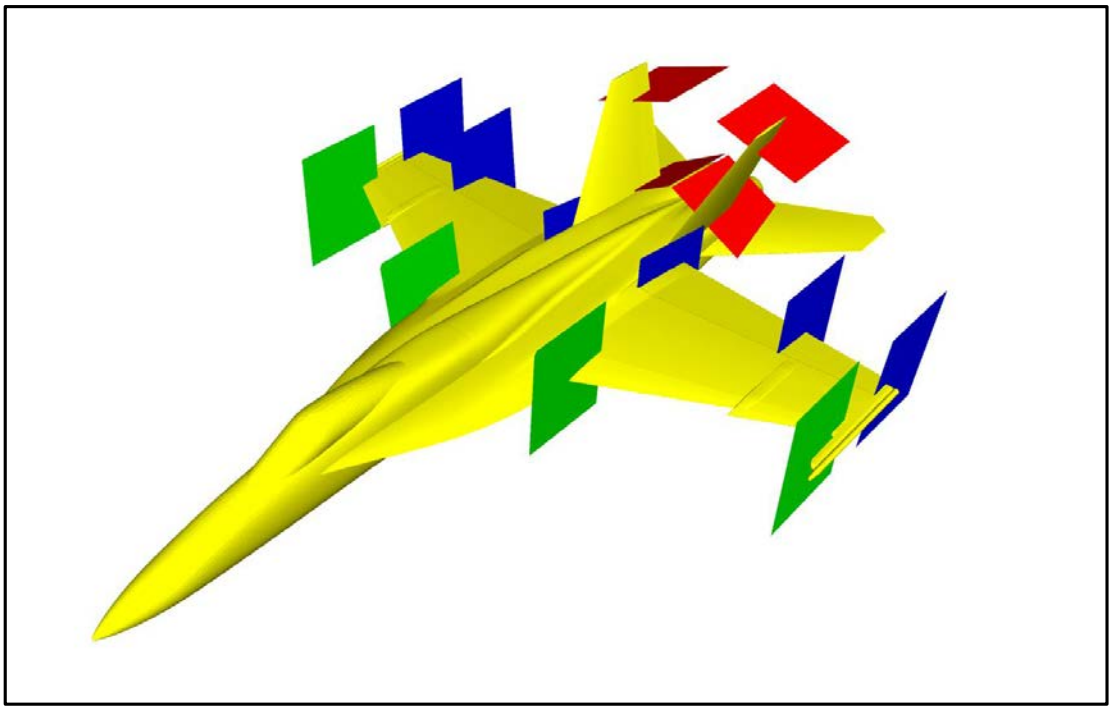

Figure 4: Interface Planes Used in the F/A-18E Grids for the Pitch/Roll/Yaw Doublet L/R SASS, Pitch Captures, 1-g Full-Stick Roll, and Constant-g WUT Maneuvers

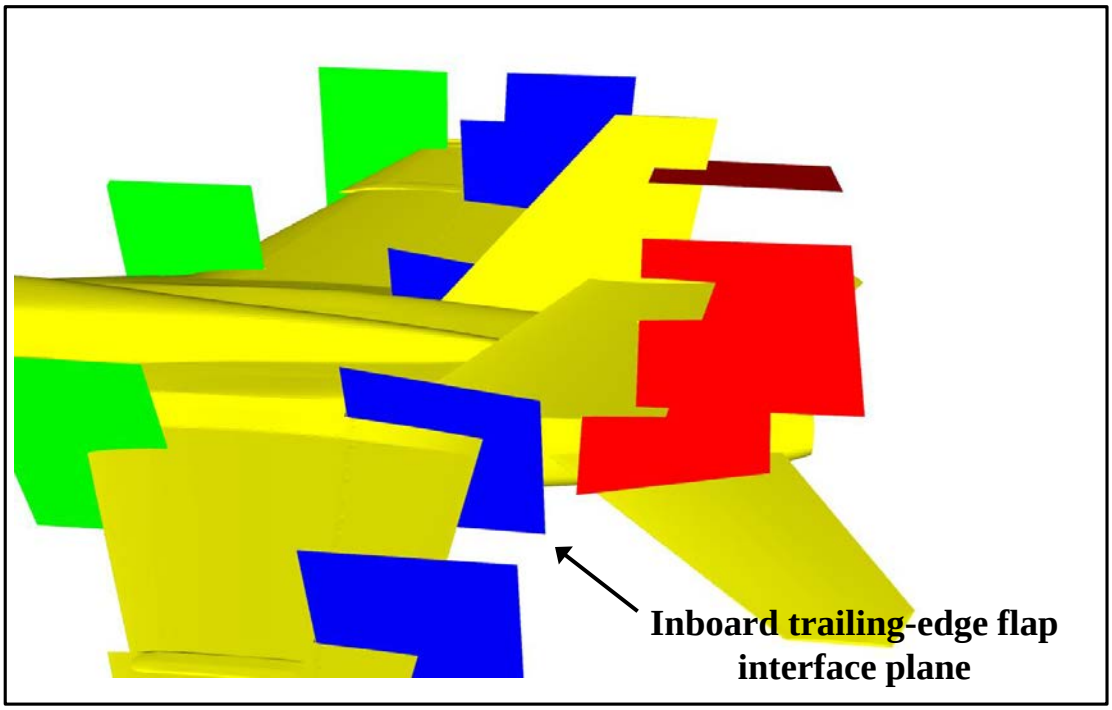

Figure 5: Second View of Interface Planes Used in the F/A-18E Grids for the Pitch/Roll/Yaw Doublet L/R SASS, Pitch Captures, 1-g Full-Stick Roll, and Constant-g WUT Maneuvers

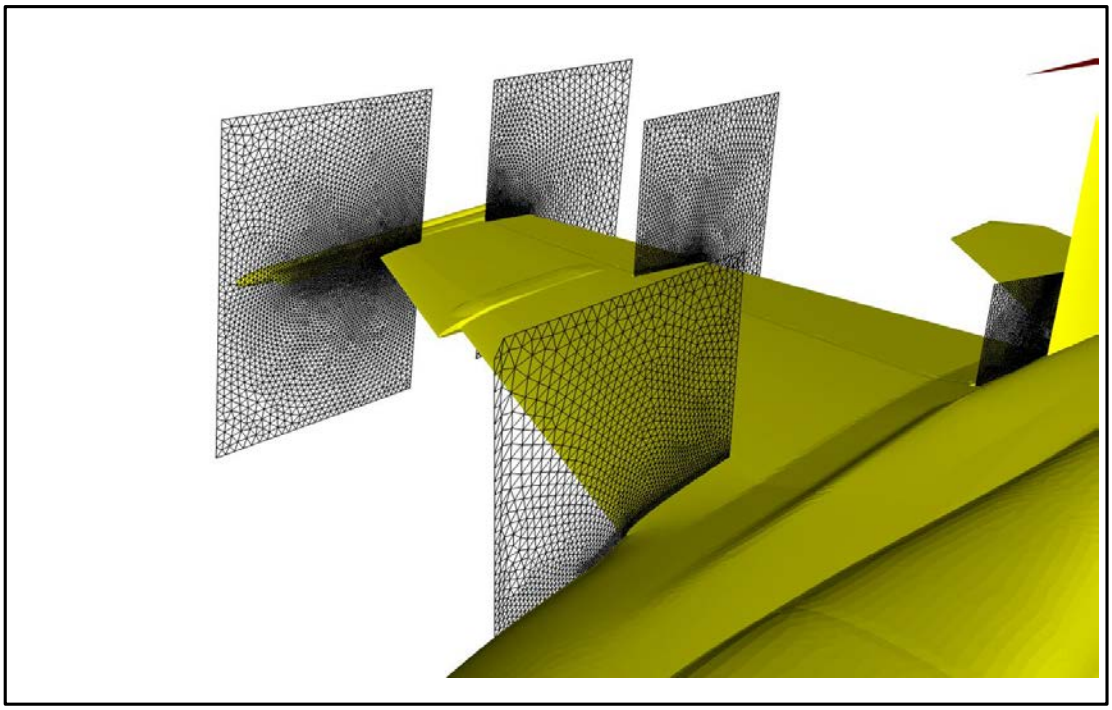

Figure 6: Grids on the Interface Planes Used in the F/A-18E Calculations for the Pitch/Roll/Yaw Doublet L/R SASS, Pitch Captures, 1-G Full-Stick Roll, and Constant-g WUT Maneuvers

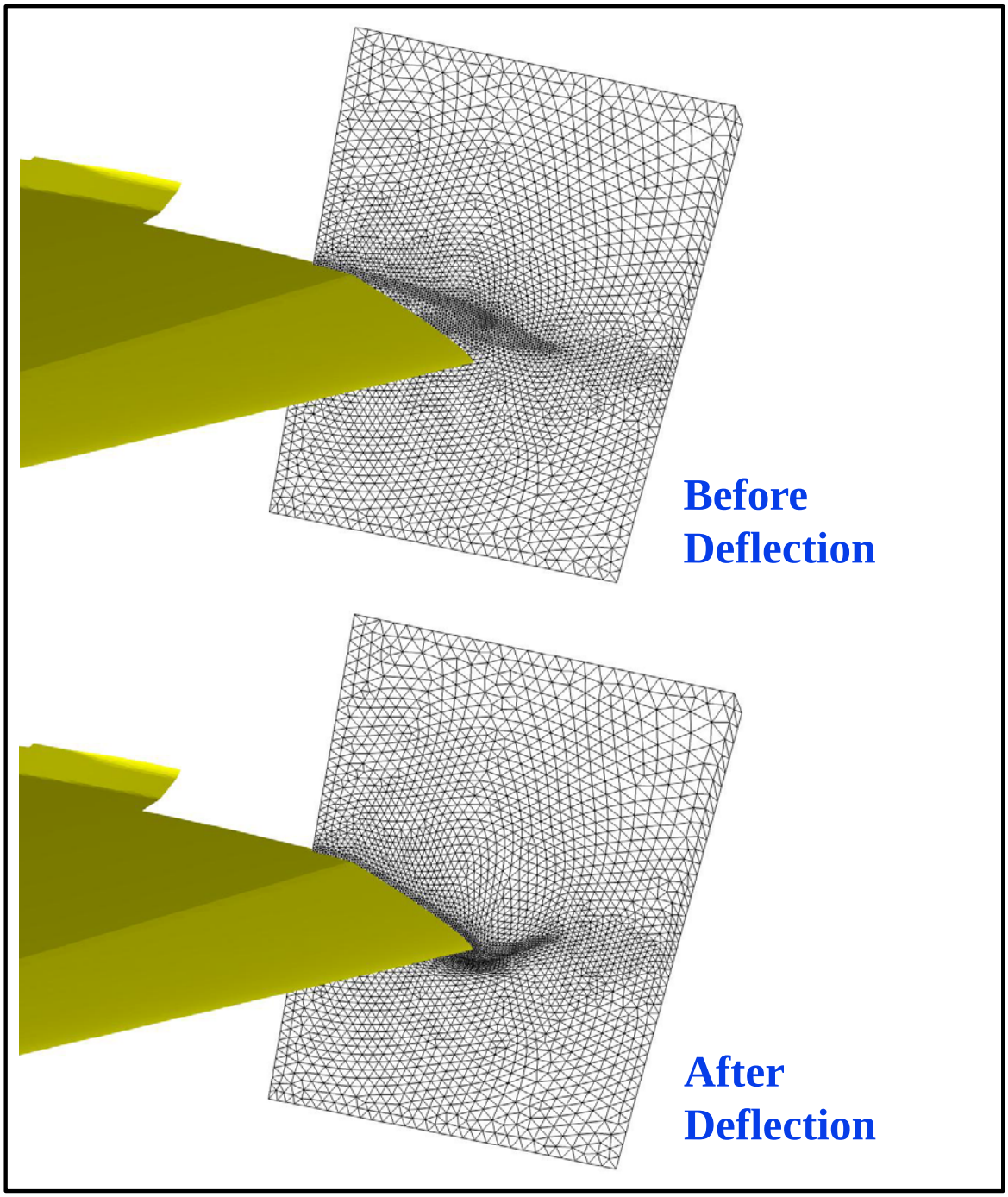

Figure 7: An Image of the Grid on the Inboard LEF Interface Plane before and after the Deflection of the Leading-Edge

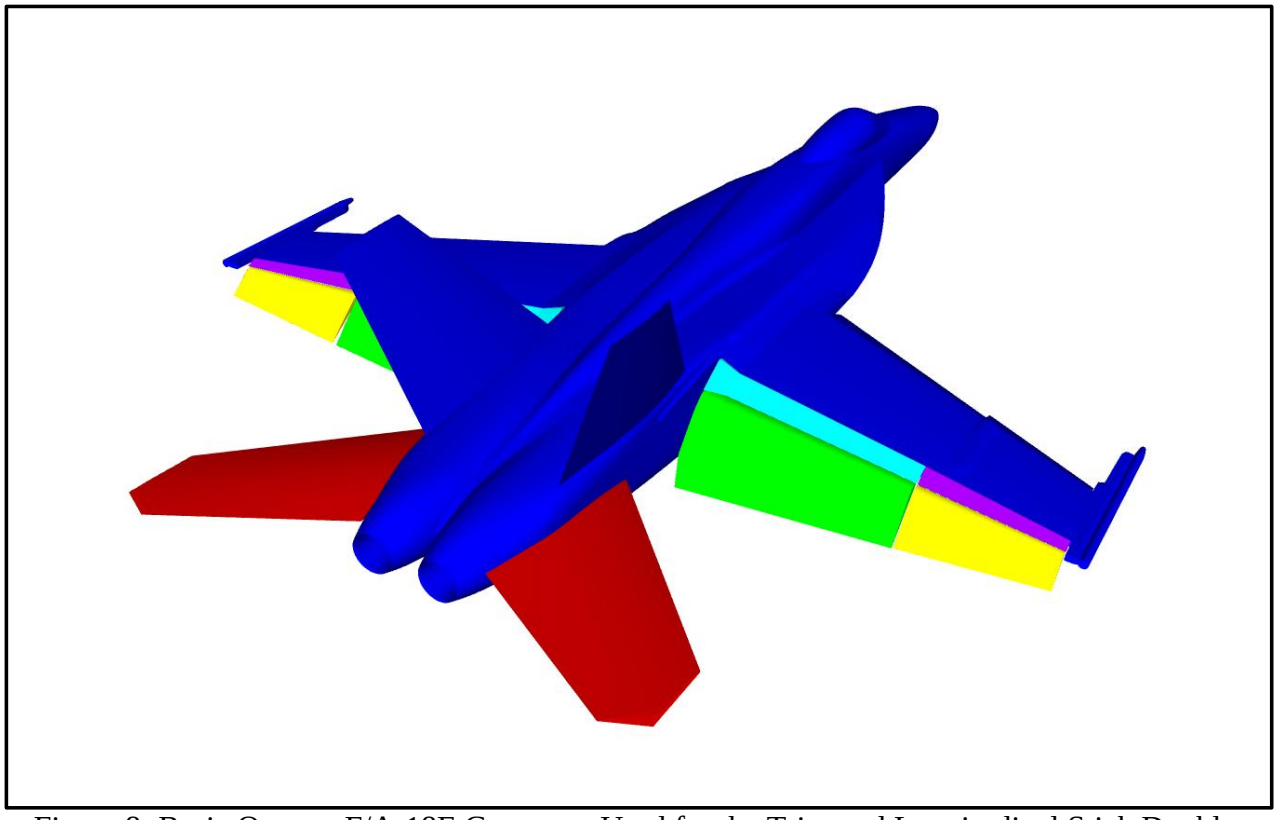

Figure 8: Basic Overset F/A-18E Geometry Used for the Trimmed Longitudinal Stick Doublet Maneuver

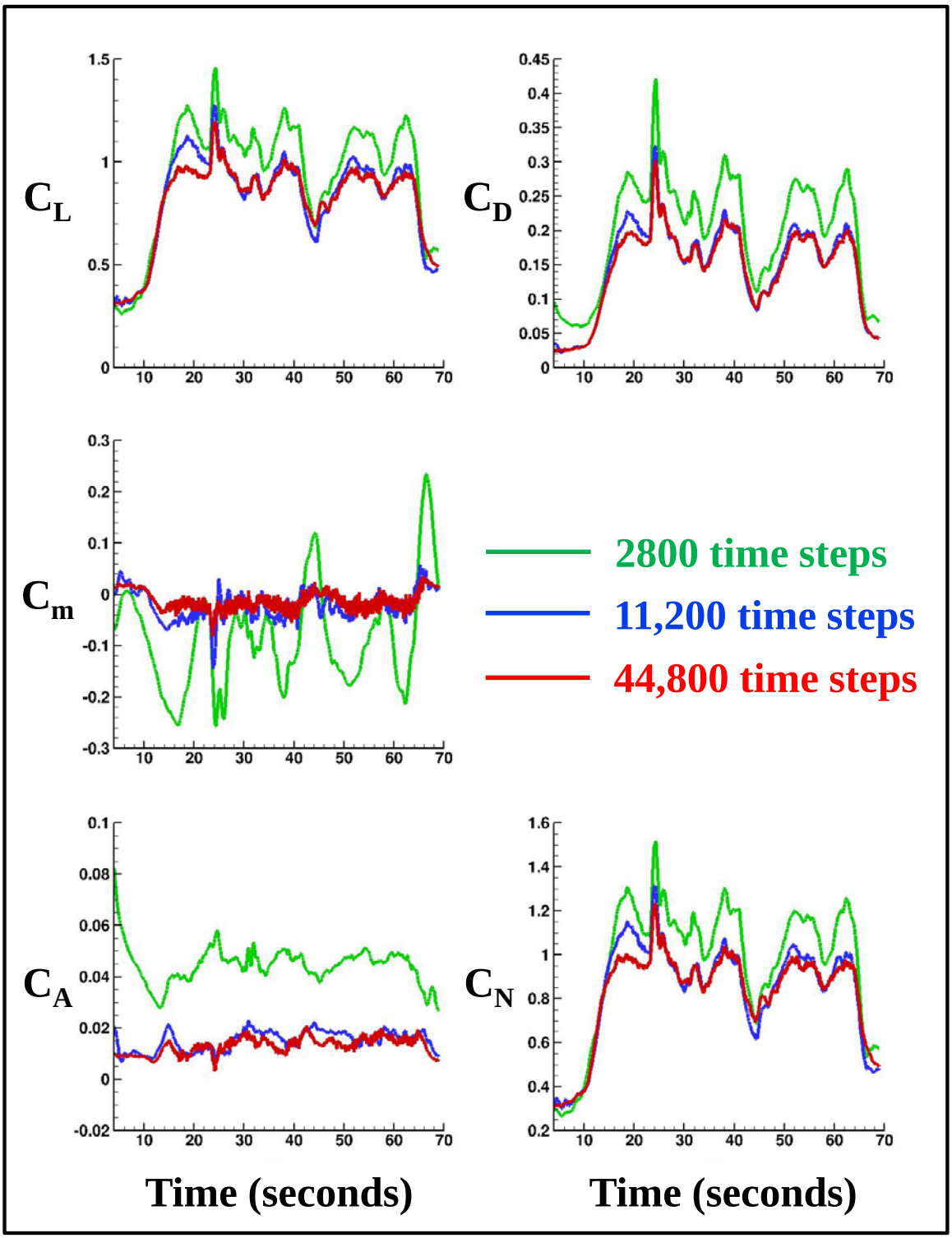

Figure 9: Results of Longitudinal Force and Moment Coefficients from Time-Step Study for the F/A-18E Pitch/Roll/Yaw Doublet L/R SASS Maneuver at Mach 0.816 and an Altitude of 34,400 ft

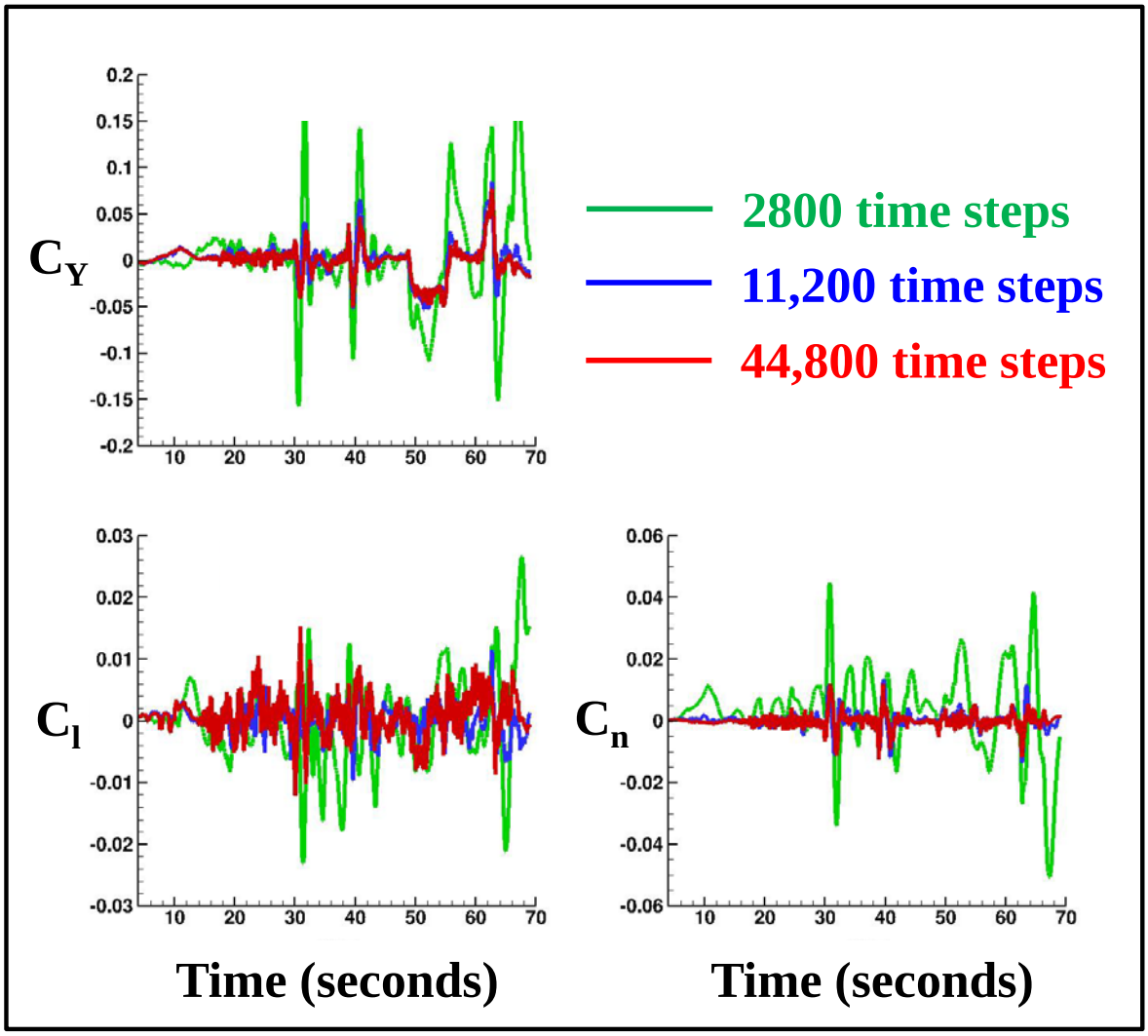

Figure 10: Results of Lateral/Directional Force and Moment Coefficients from Time-Step Study for the F/A-18E Pitch/Roll/Yaw Doublet L/R SASS Maneuver at Mach 0.816 and an Altitude of 34,400 ft

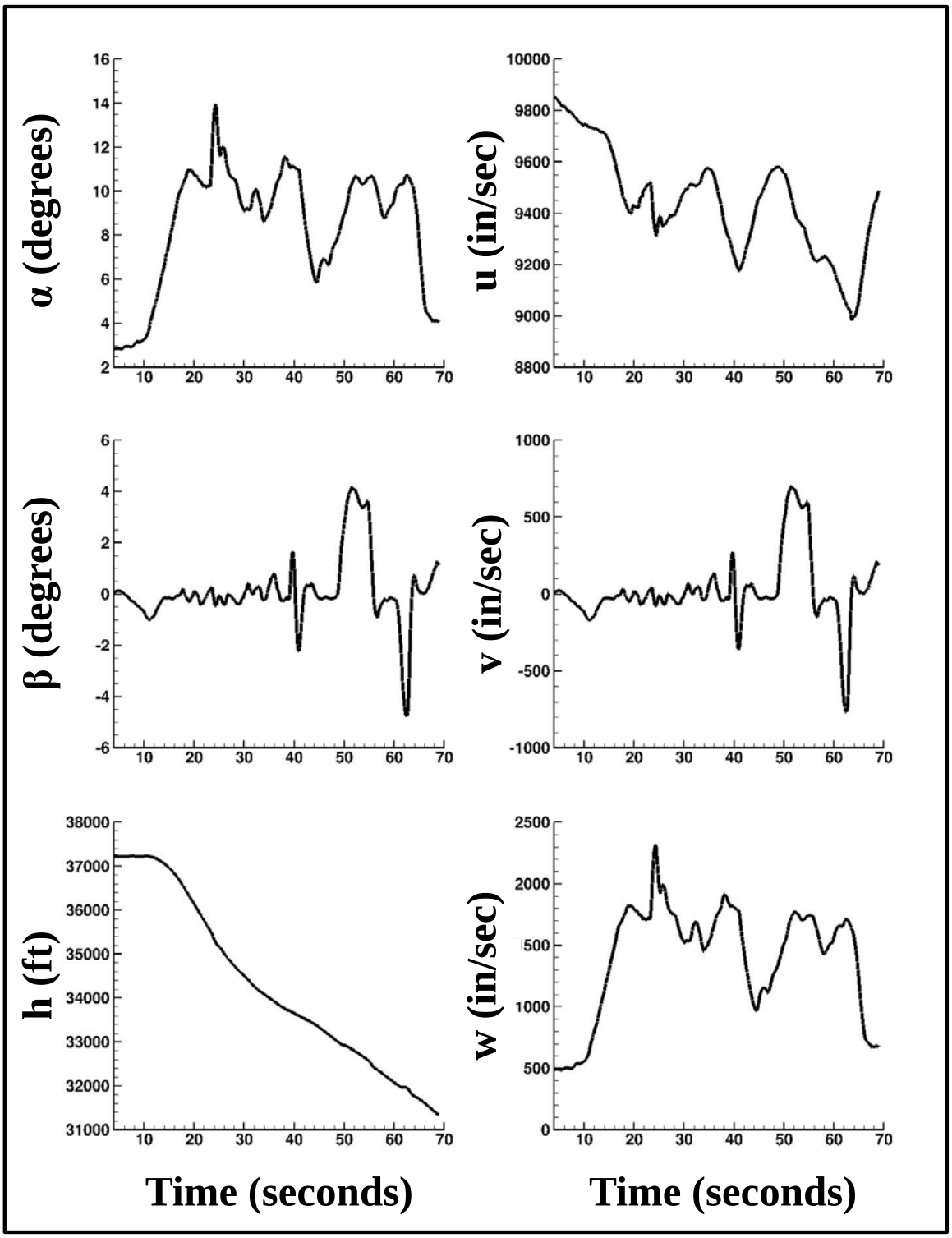

Figure 11: AOA, AOSS, Altitude, u-, v- and w-Velocity Components for the F/A-18E Pitch/Roll/Yaw Doublet L/R SASS Maneuver

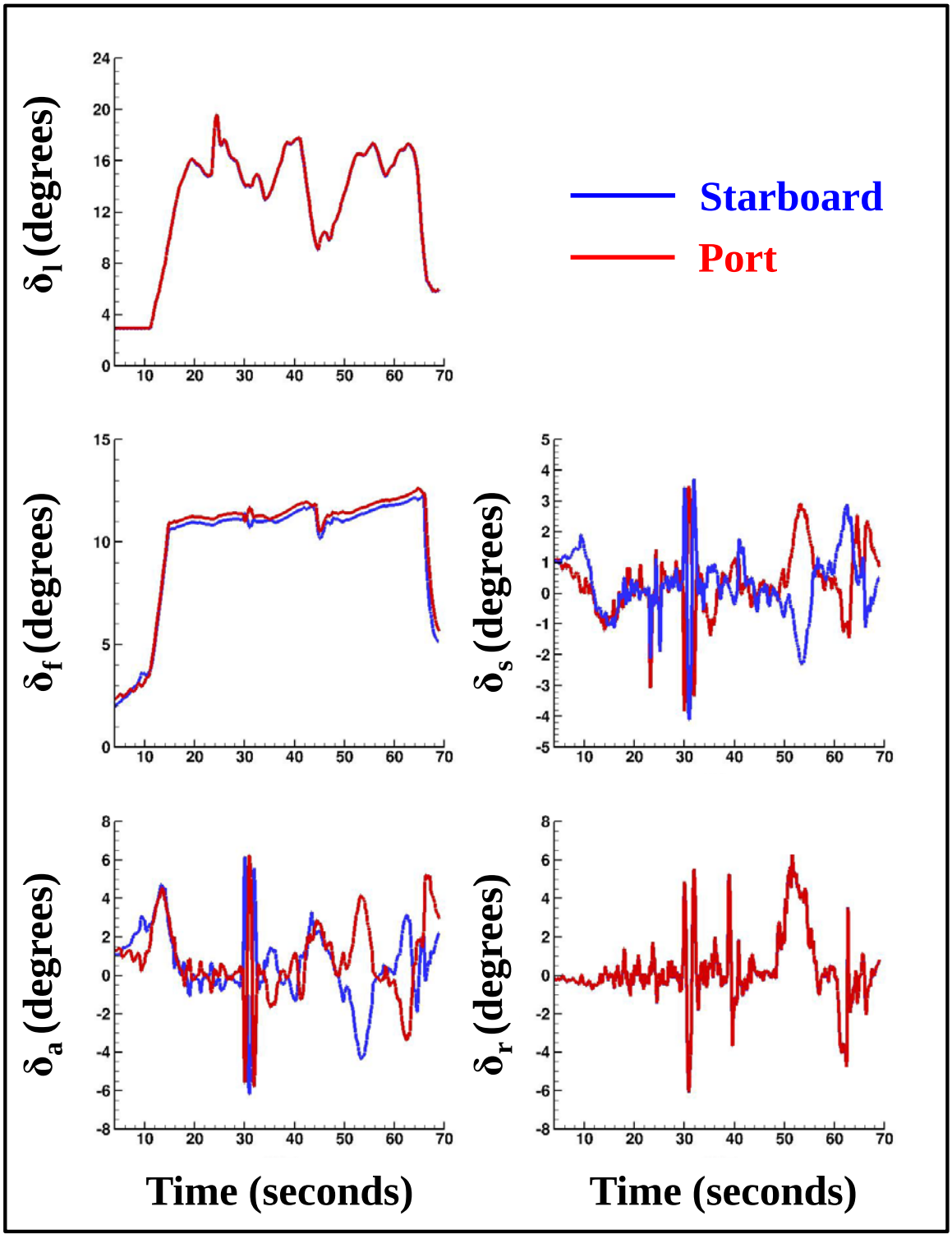

Figure 12: LEF, TEF, Aileron, Horizontal-Tail, and Rudder Deflections for the F/A-18E Pitch/Roll/Yaw Doublet L/R SASS Maneuver

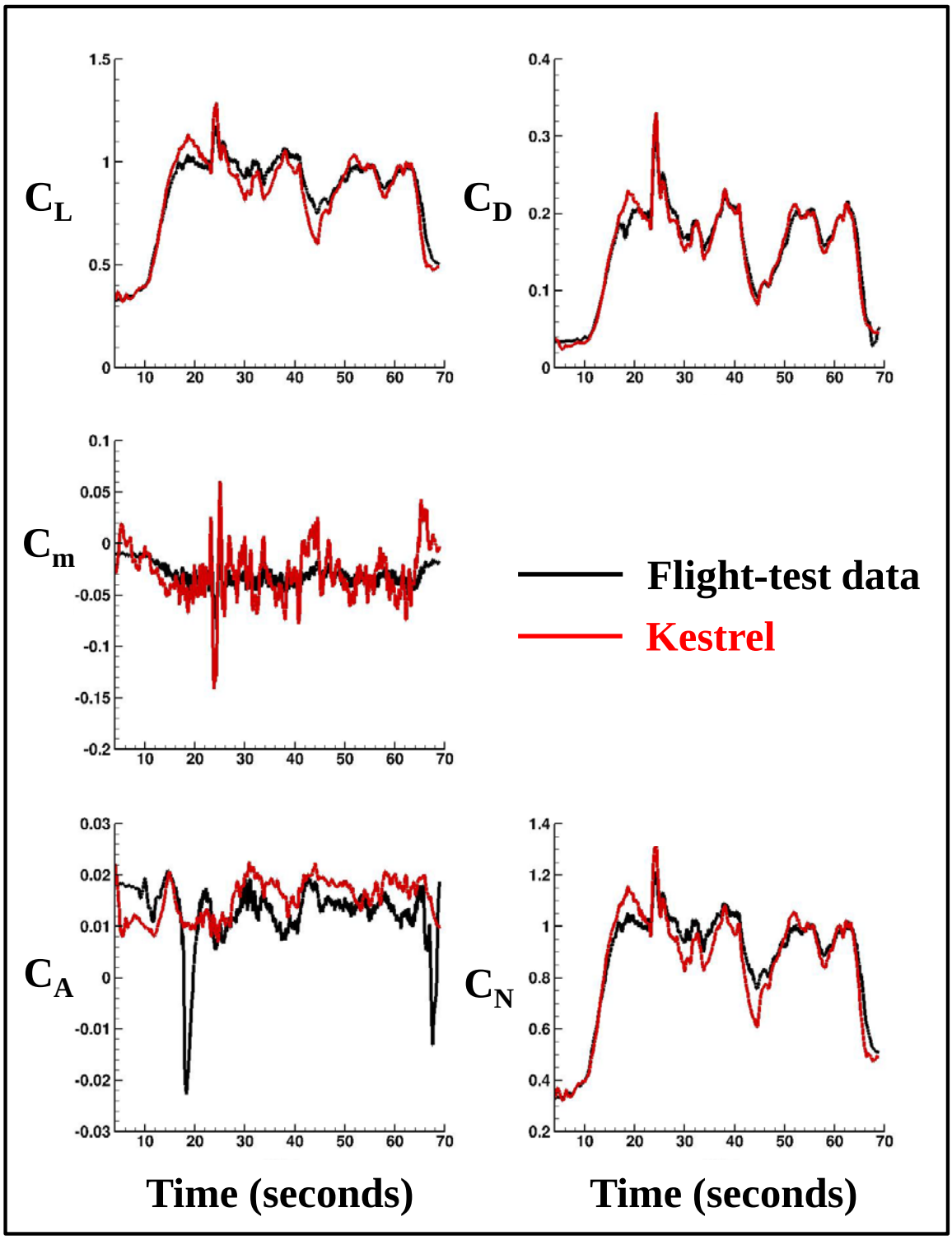

Figure 13: Longitudinal Force and Moment Coefficients for Kestrel and Flight-Test Data for the F/A-18E Pitch/Roll/Yaw Doublet L/R SASS Maneuver at Mach 0.816 and an Altitude of 34,400 ft

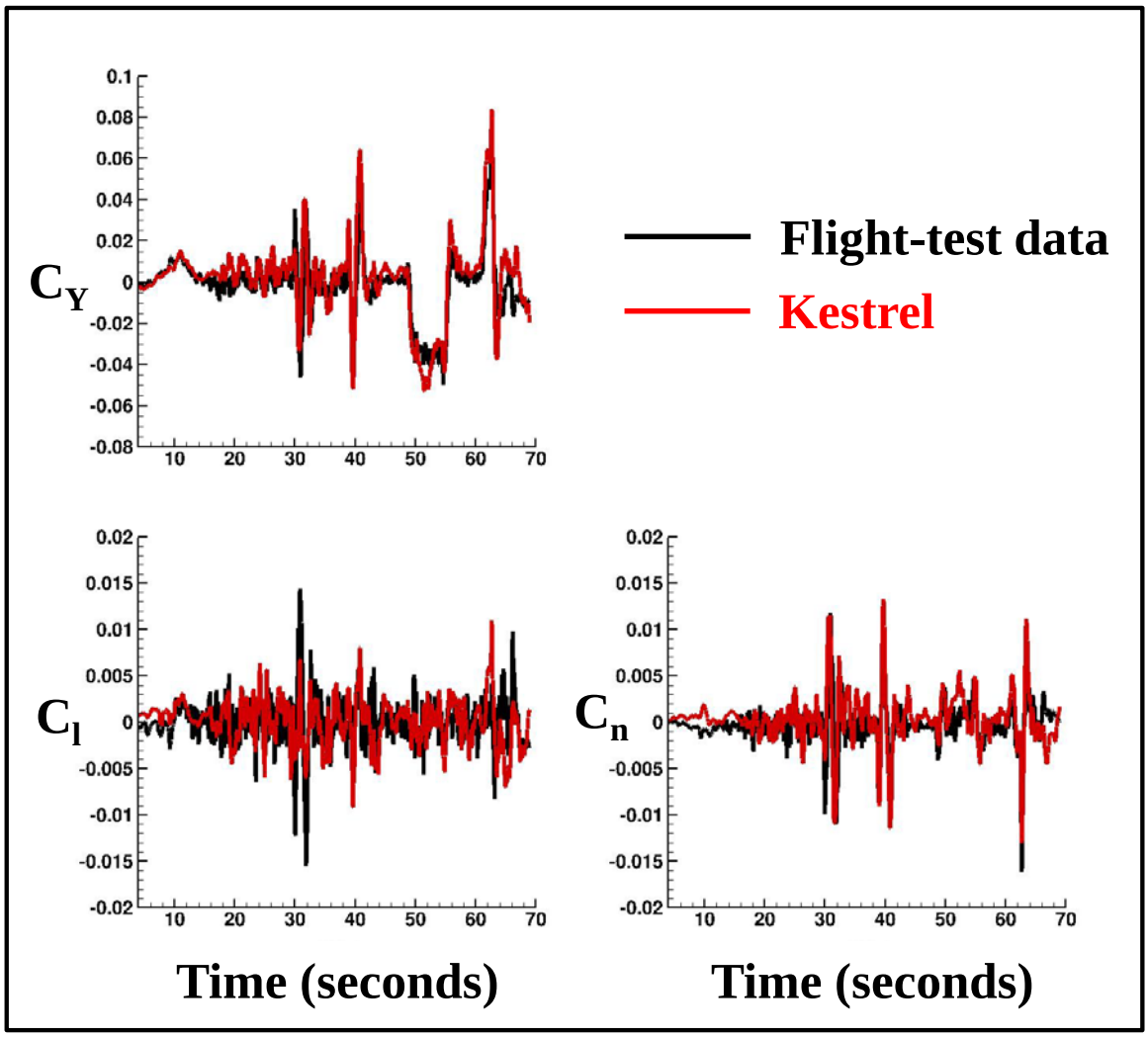

Figure 14: Lateral/Directional Force and Moment Coefficients for Kestrel and Flight-Test Data for the F/A-18E Pitch/Roll/Yaw Doublet L/R SASS Maneuver at Mach 0.816 and an Altitude of 34,400 ft

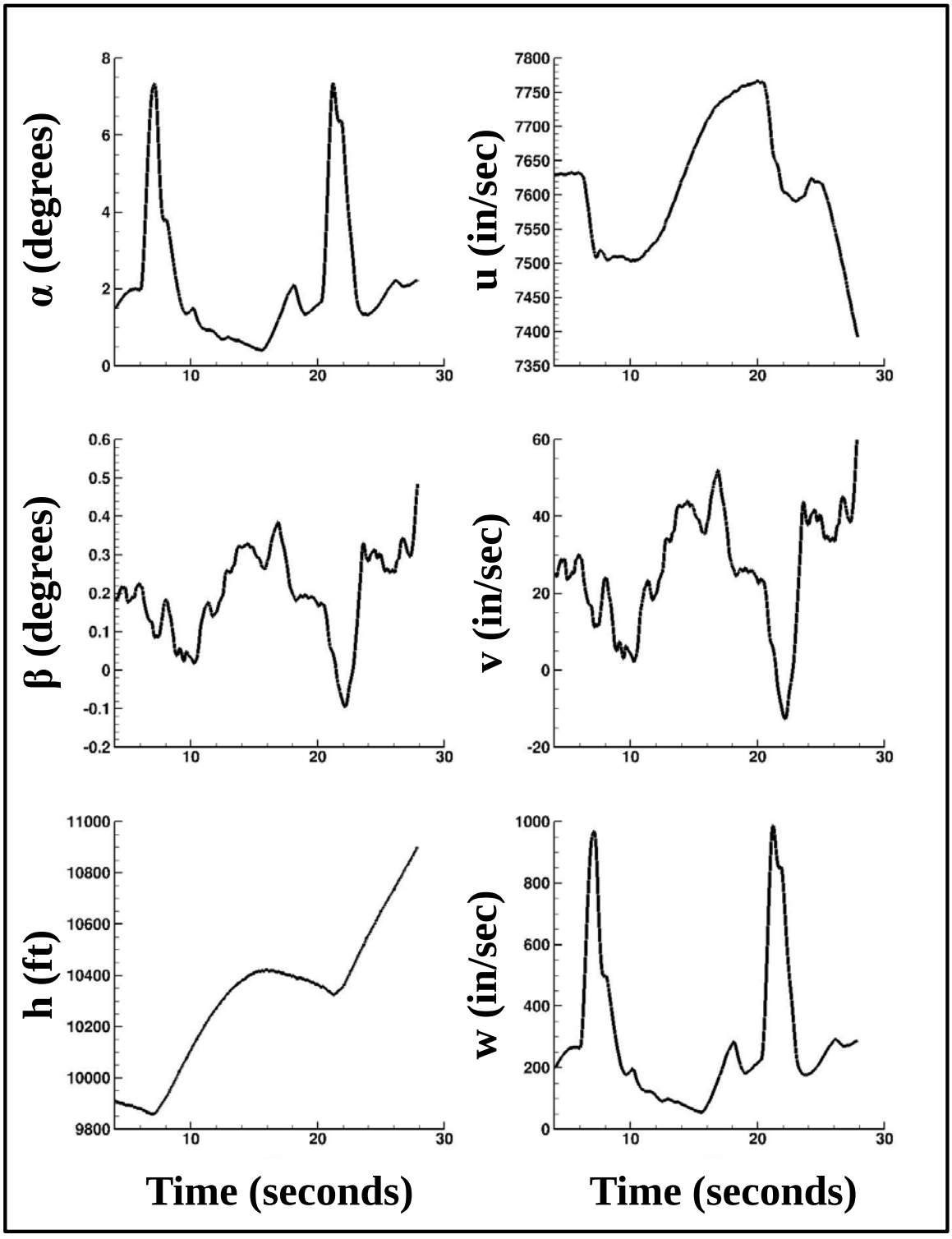

Figure 15: AOA, AOSS, Altitude, u-, v- and w-Velocity Components for the F/A-18E Pitch Captures Maneuver

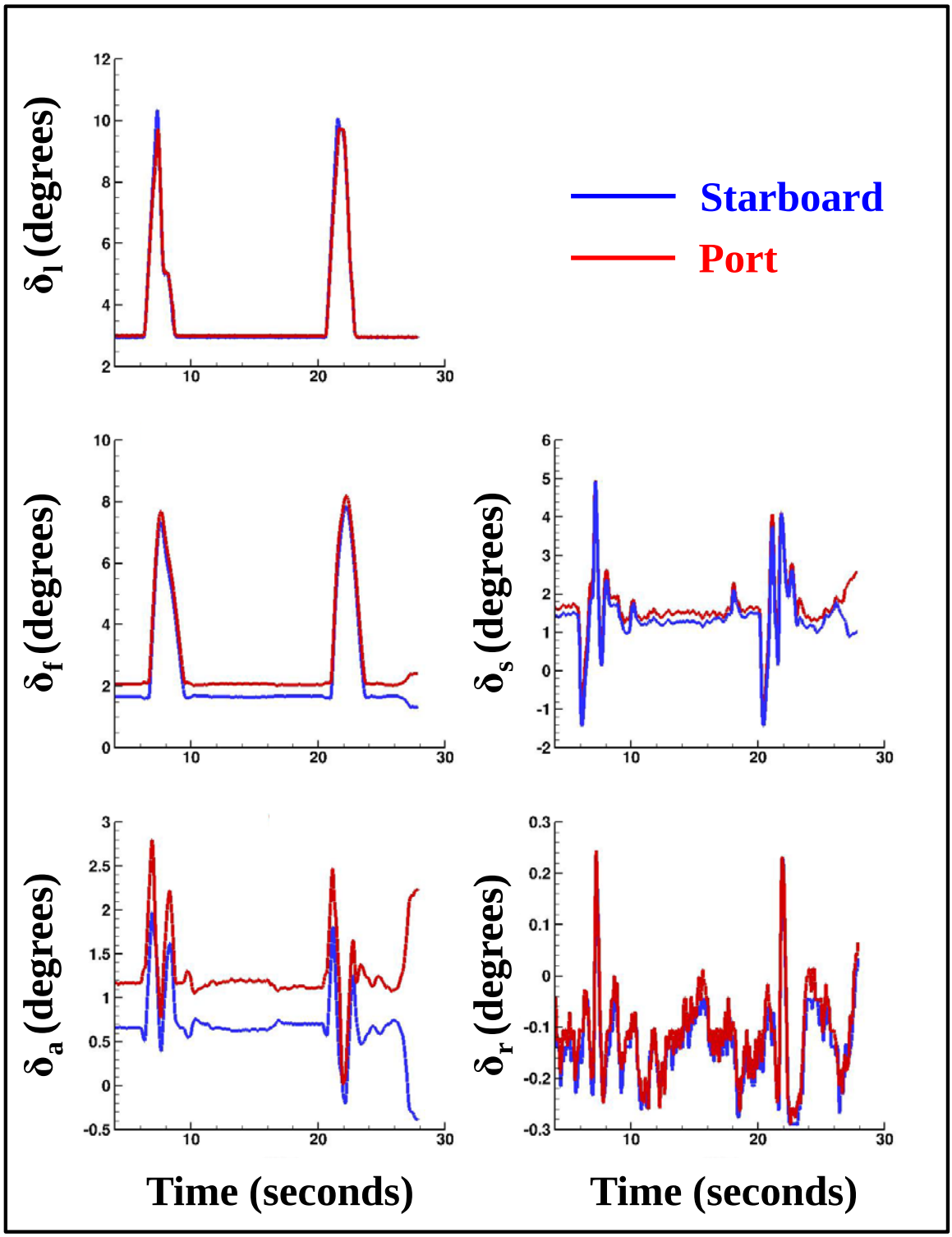

Figure 16: LEF, TEF, Aileron, Horizontal-Tail, and Rudder Deflections for the F/A-18E Pitch Captures Maneuver

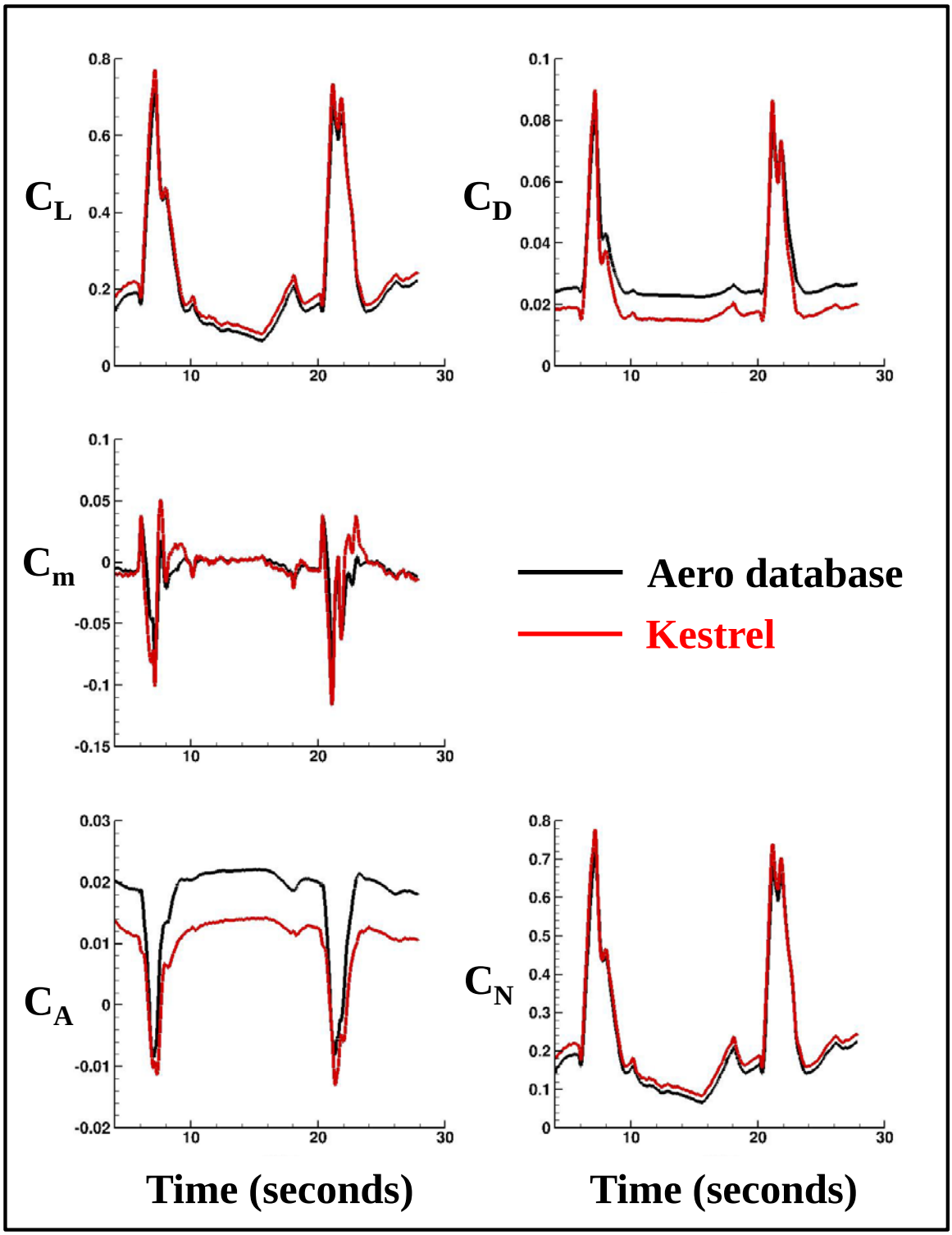

Figure 17: Longitudinal Force and Moment Coefficients for Kestrel and Aero Database for the F/A-18E Pitch Captures Maneuver at Mach 0.59 and an Altitude of 10,300 ft

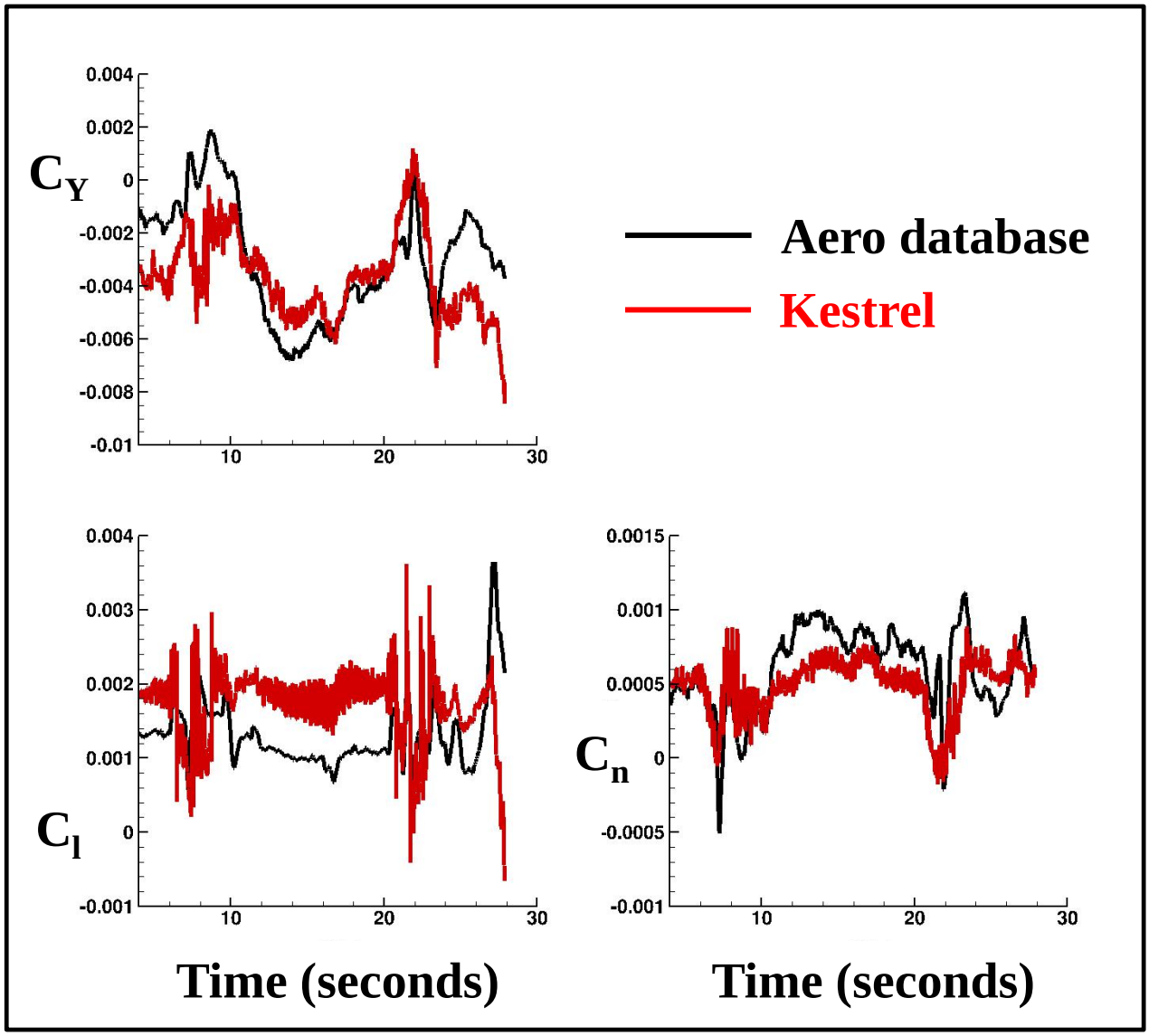

Figure 18: Lateral/Directional Force and Moment Coefficients for Kestrel and Aero Database for the F/A-18E Pitch Captures Maneuver at Mach 0.59 and an Altitude of 10,300 ft

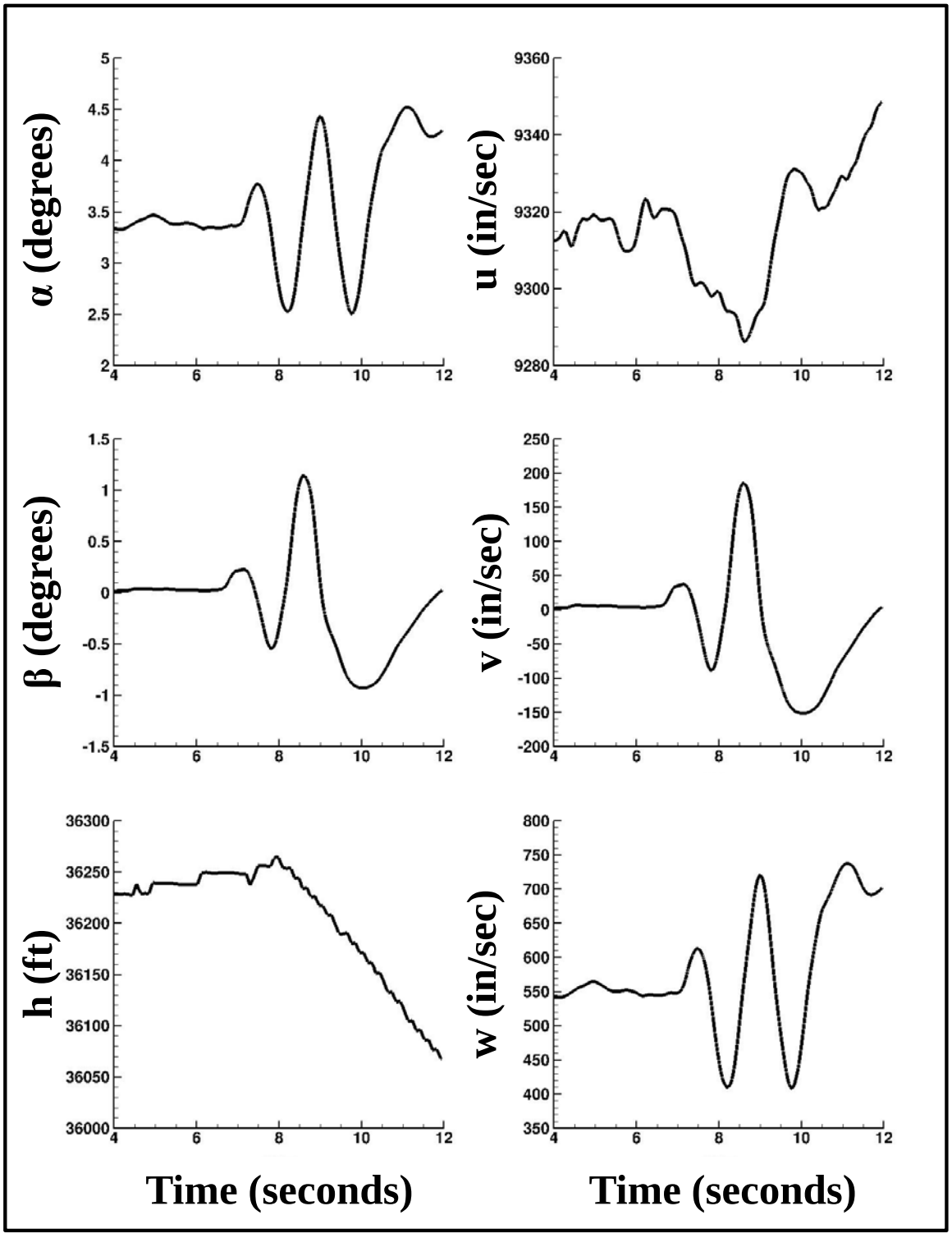

Figure 19: AOA, AOSS, Altitude, u-, v- and w-Velocity Components for the F/A-18E 1-g Full-Stick Roll Maneuver

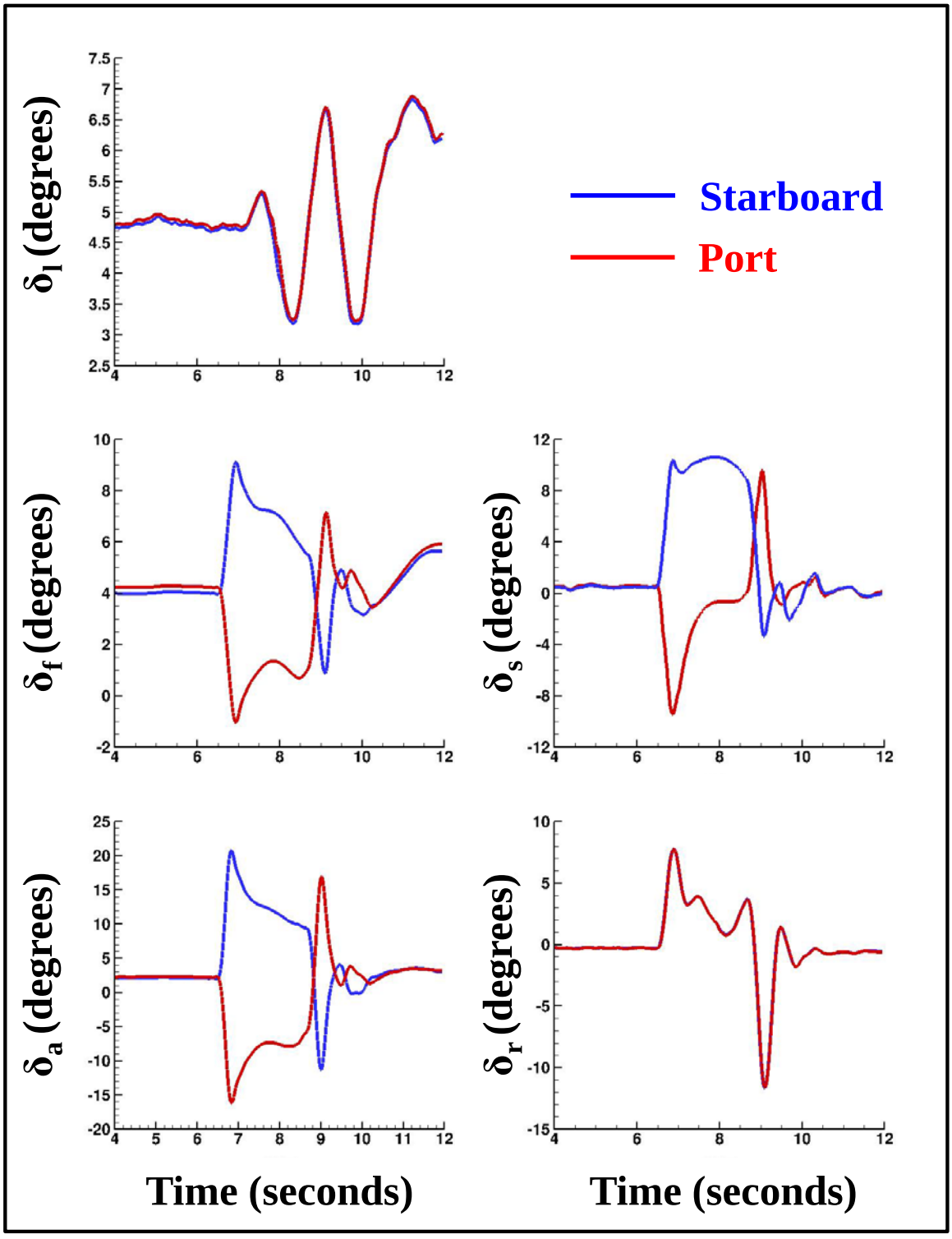

Figure 20: LEF, TEF, Aileron, Horizontal-Tail and Rudder Deflections for the F/A-18E 1-g Full-Stick Roll Maneuver

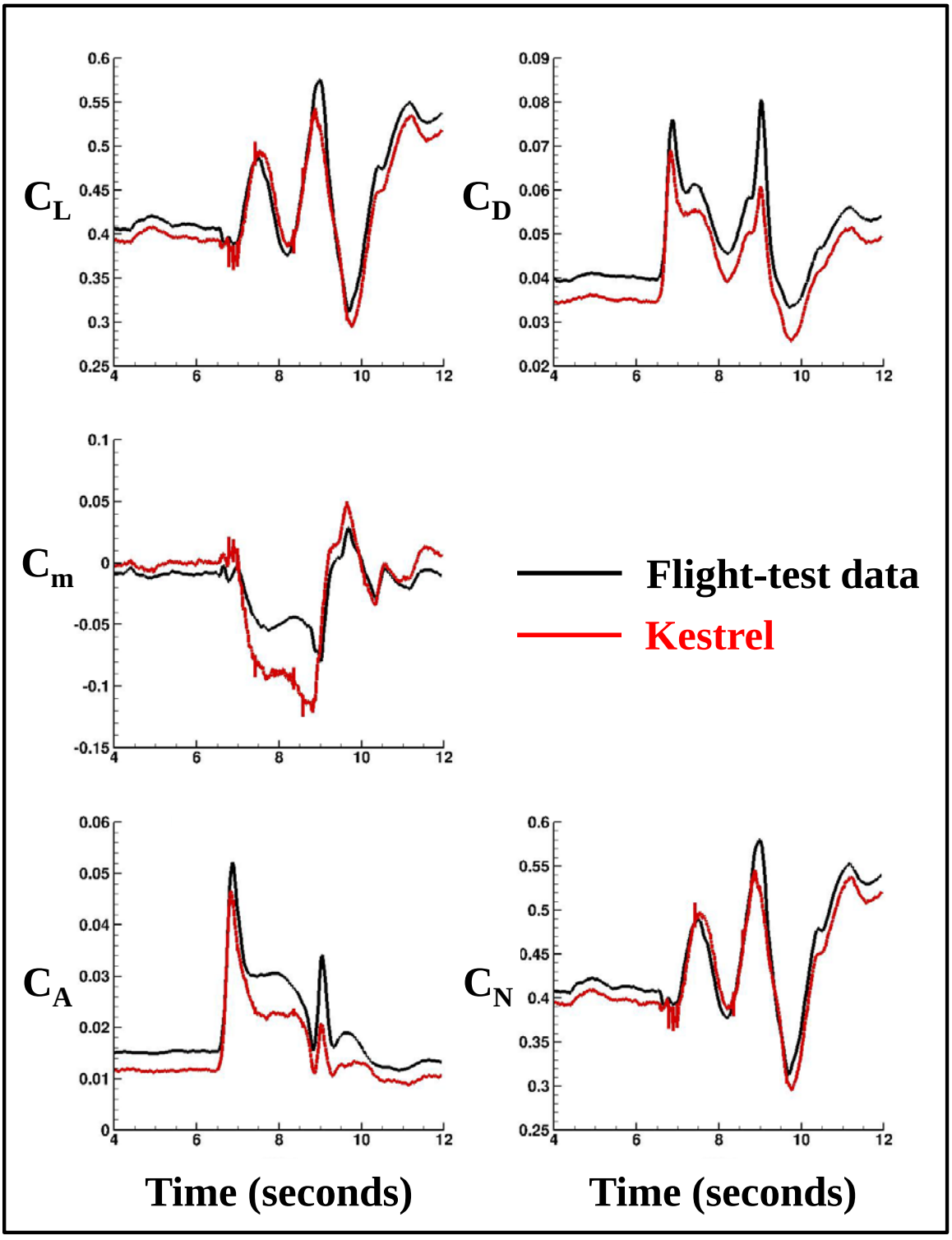

Figure 21: Longitudinal Force and Moment Coefficients for Kestrel and Flight-Test Data for the F/A-18E 1-g Full-Stick Roll Maneuver at Mach 0.804 and an Altitude of 36,200 ft

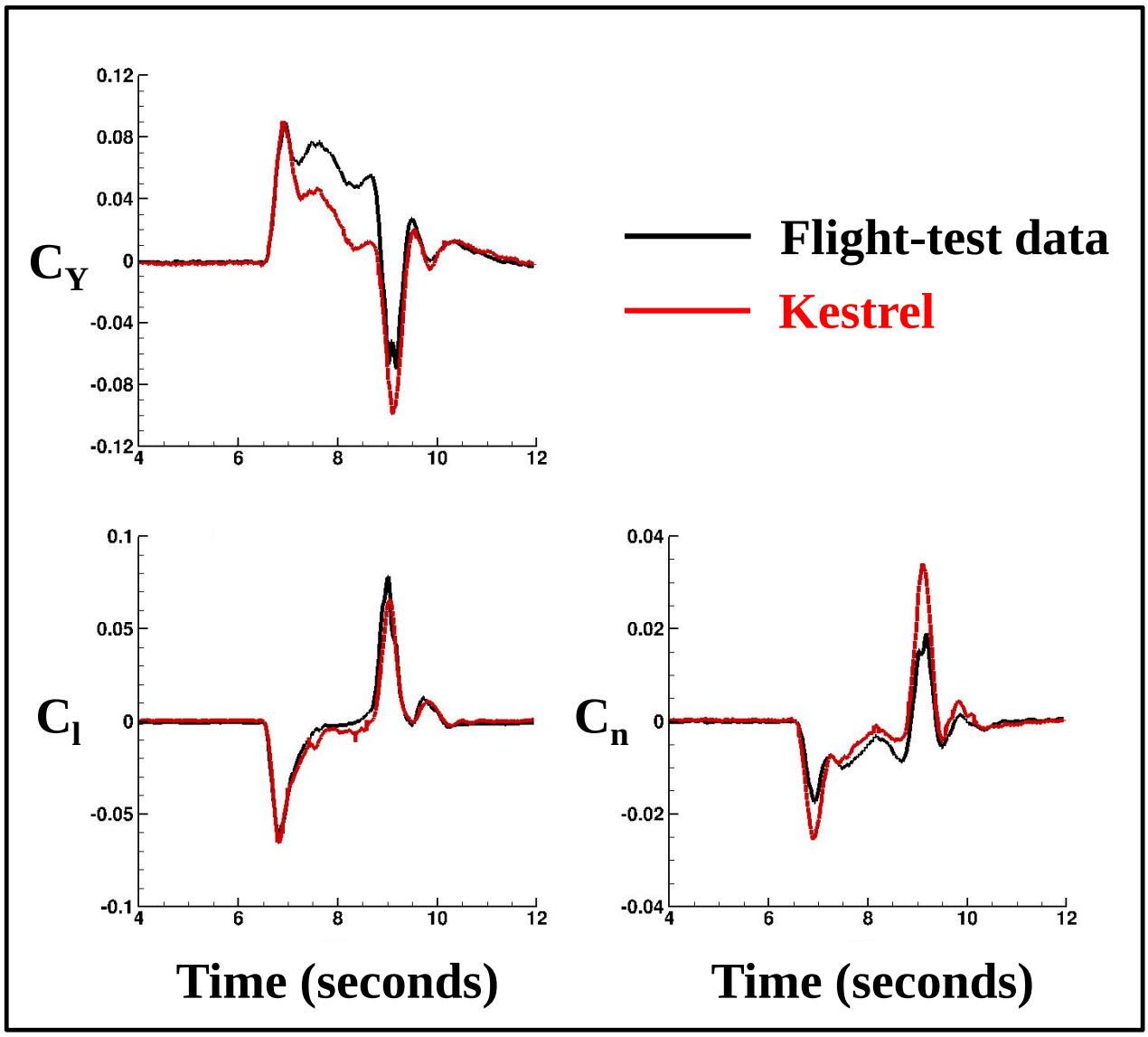

Figure 22: Lateral/Directional Force and Moment Coefficients for Kestrel and Flight-Test Data for the F/A-18E 1-g Full-Stick Roll Maneuver at Mach 0.804 and an Altitude of 36,200 ft

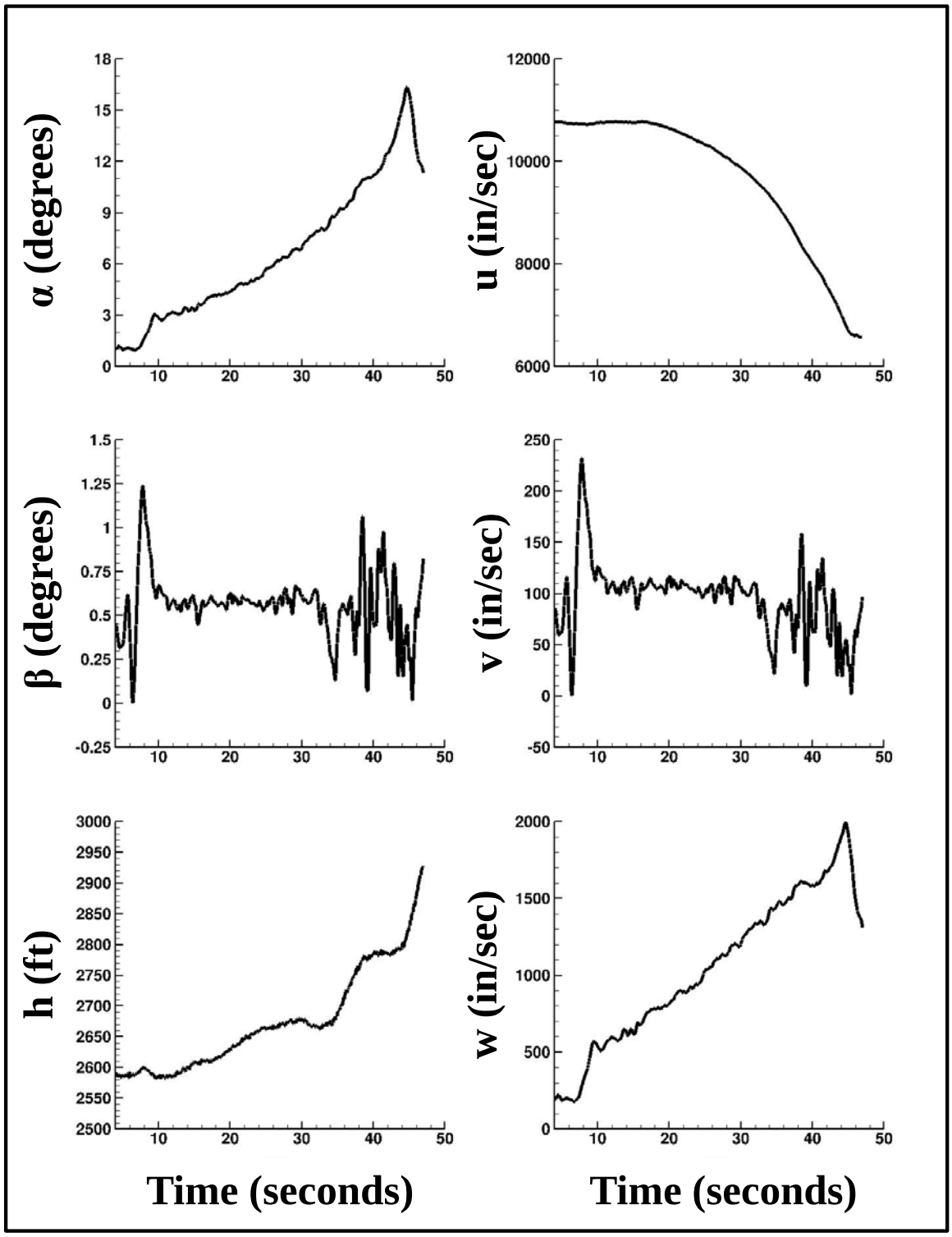

Figure 23: AOA, AOSS, Altitude, u-, v- and w-Velocity Components for the F/A-18E Constant-g WUT Maneuver

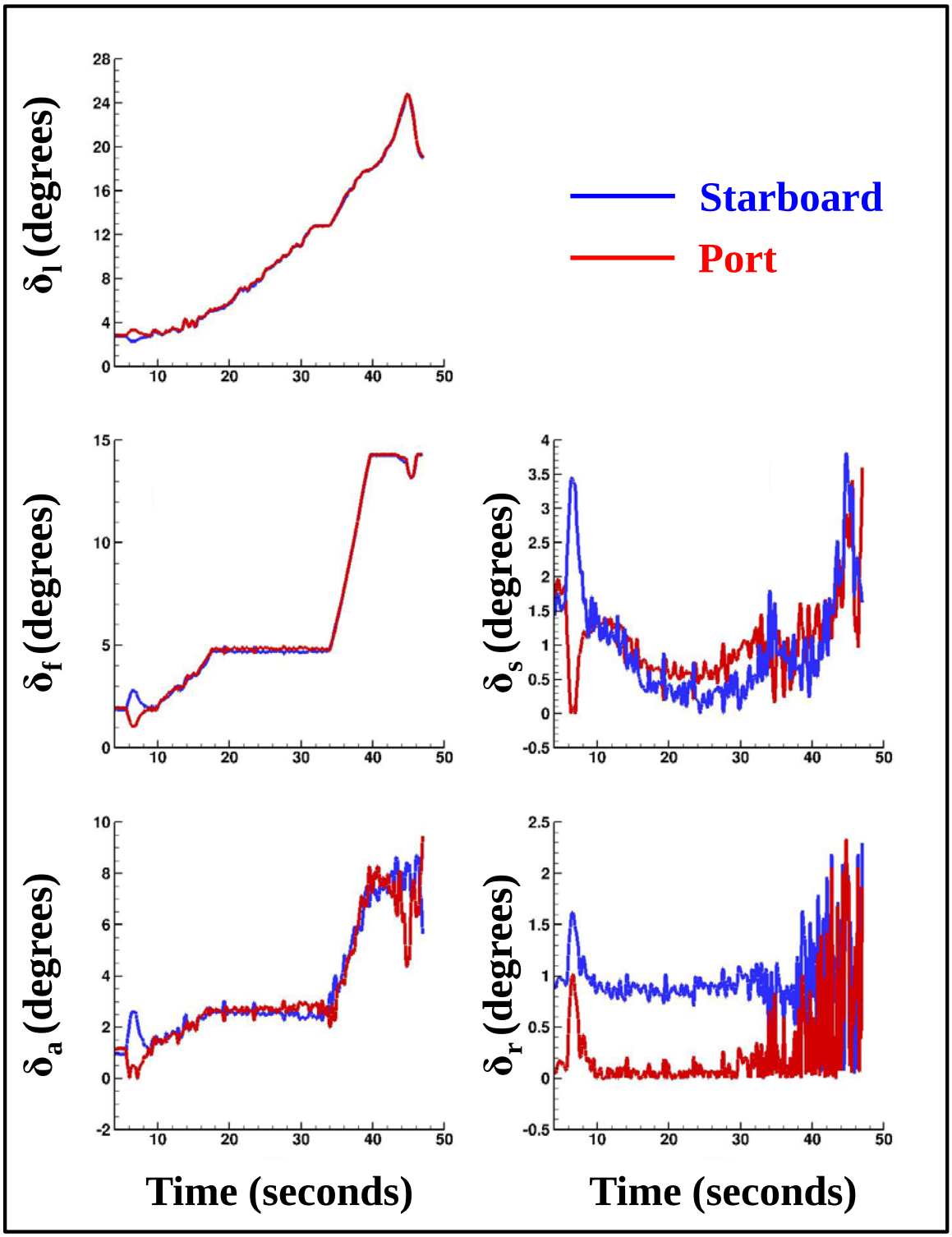

Figure 24: LEF, TEF, Aileron, Horizontal-Tail and Rudder Deflections for the F/A-18E Constant-g WUT Maneuver

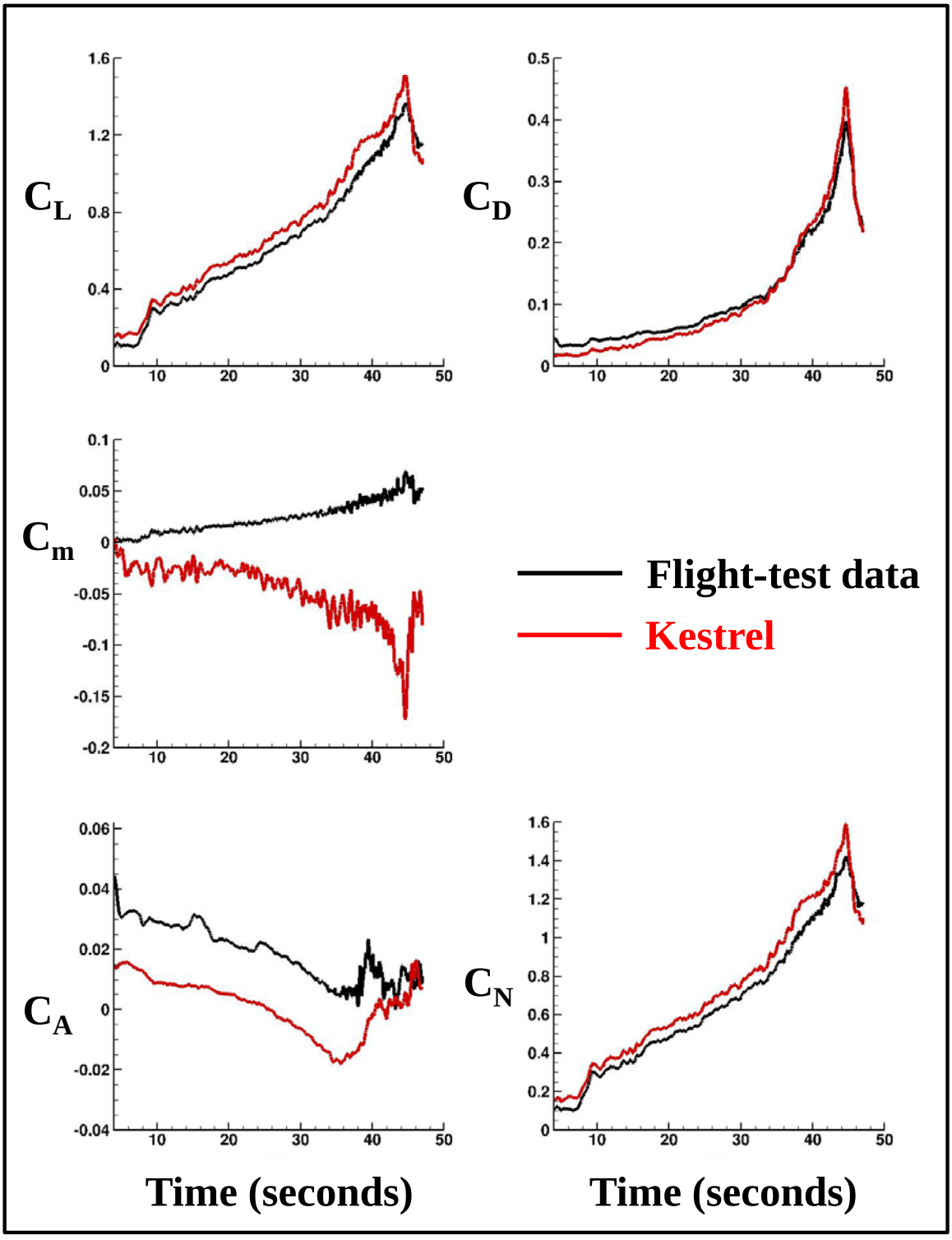

Figure 25: Longitudinal Force and Moment Coefficients for Kestrel and Flight-Test Data for the F/A-18E Constant-g WUT Maneuver at Mach 0.735 and an Altitude of 2,700 ft

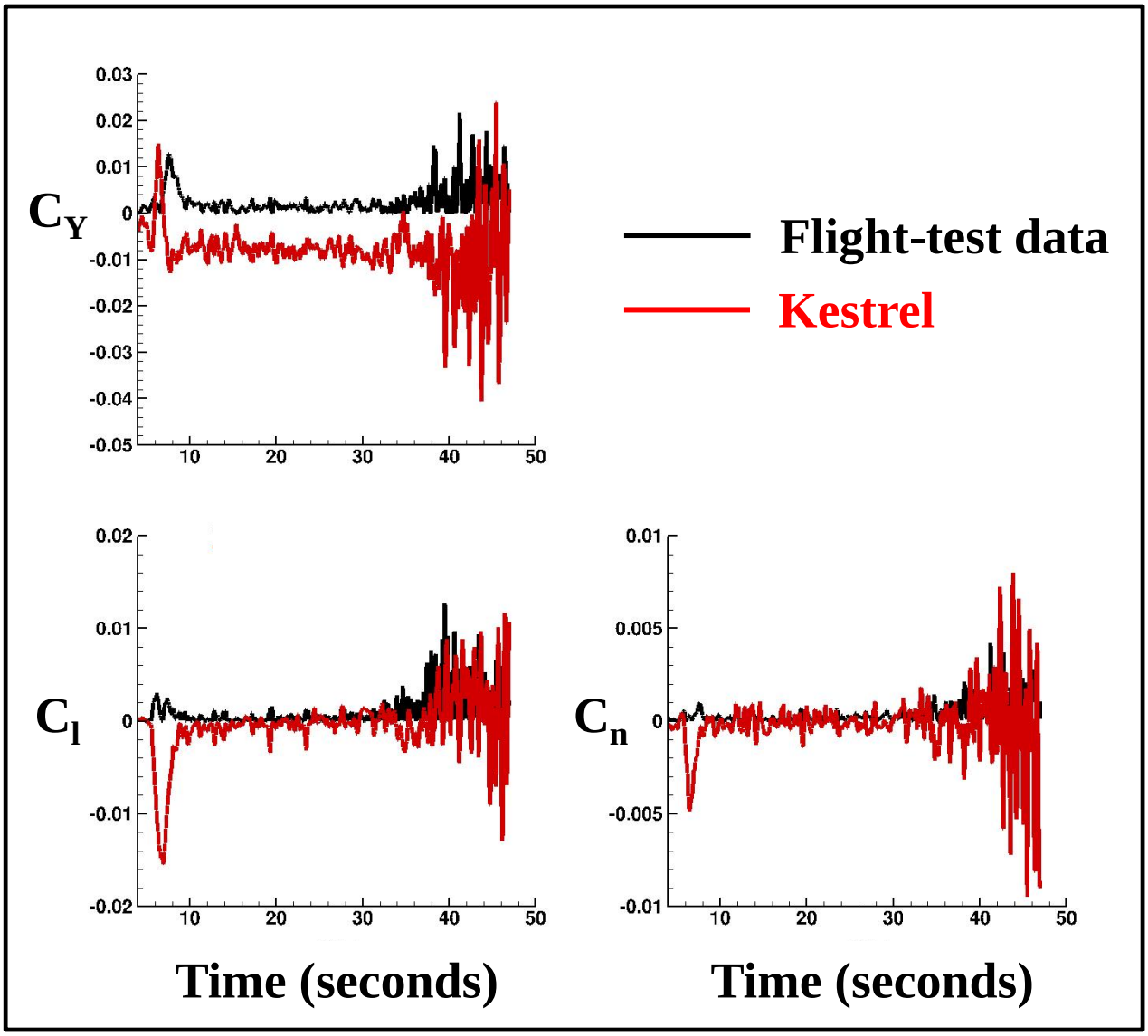

Figure 26: Lateral/Directional Force and Moment Coefficients for Kestrel and Flight-Test Data for the F/A-18E Constant-g WUT Maneuver at Mach 0.735 and an Altitude of 2,700 ft

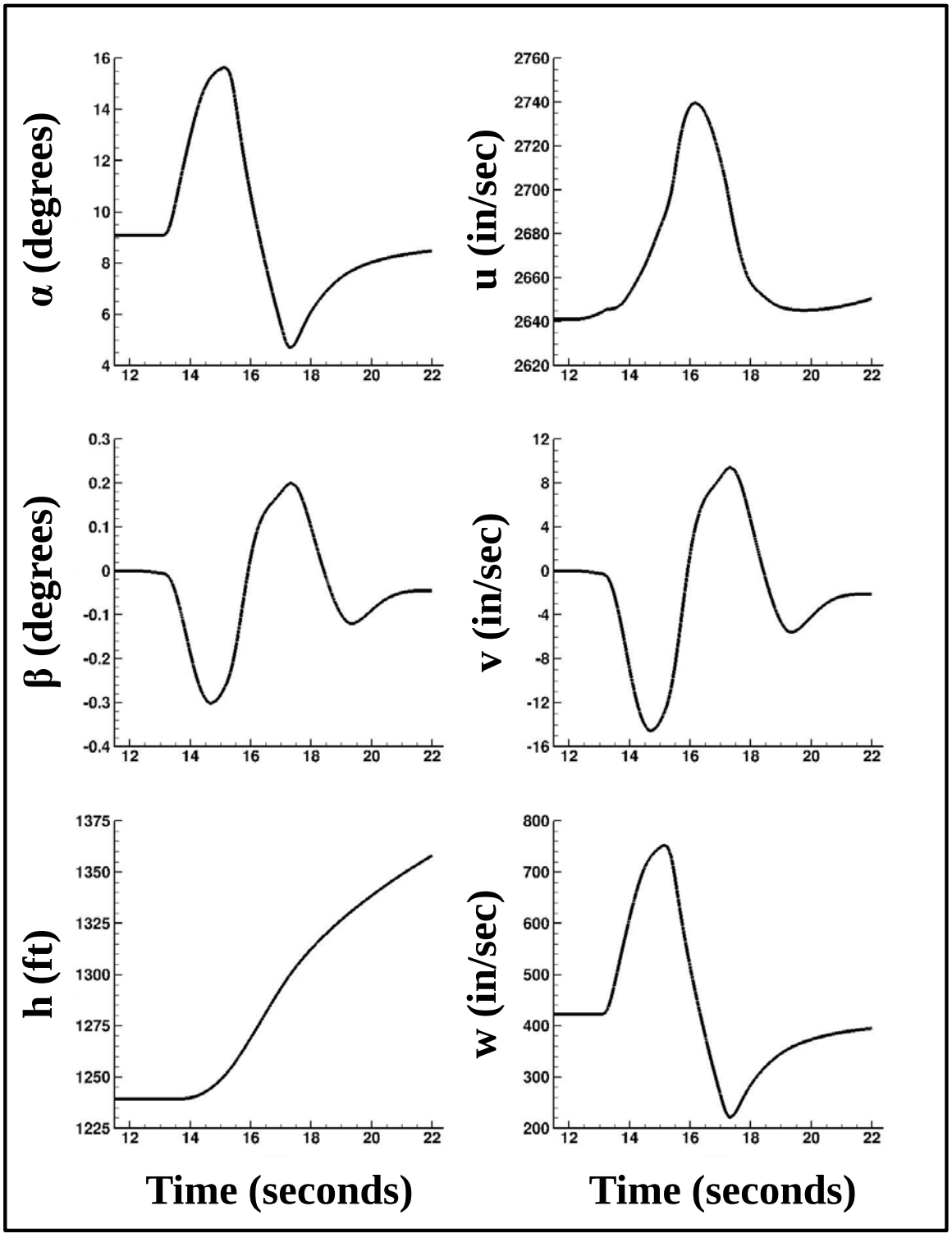

Figure 27: AOA, AOSS, Altitude, u-, v- and w-Velocity Components for the F/A-18E Trimmed Longitudinal Stick Doublet Maneuver

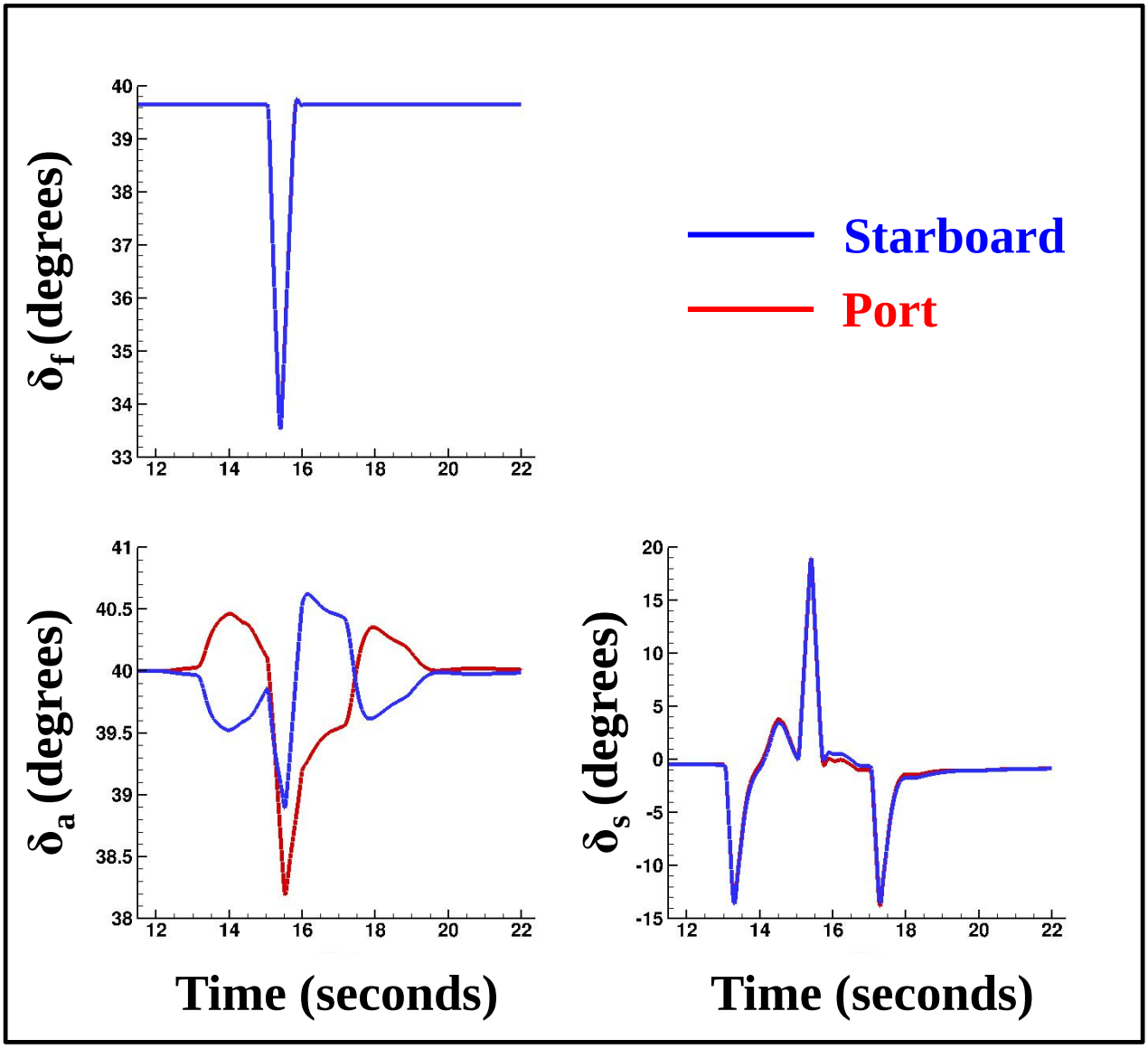

Figure 28: TEF, Aileron, and Horizontal-Tail Deflections for the F/A-18E Trimmed Longitudinal Stick Doublet Maneuver

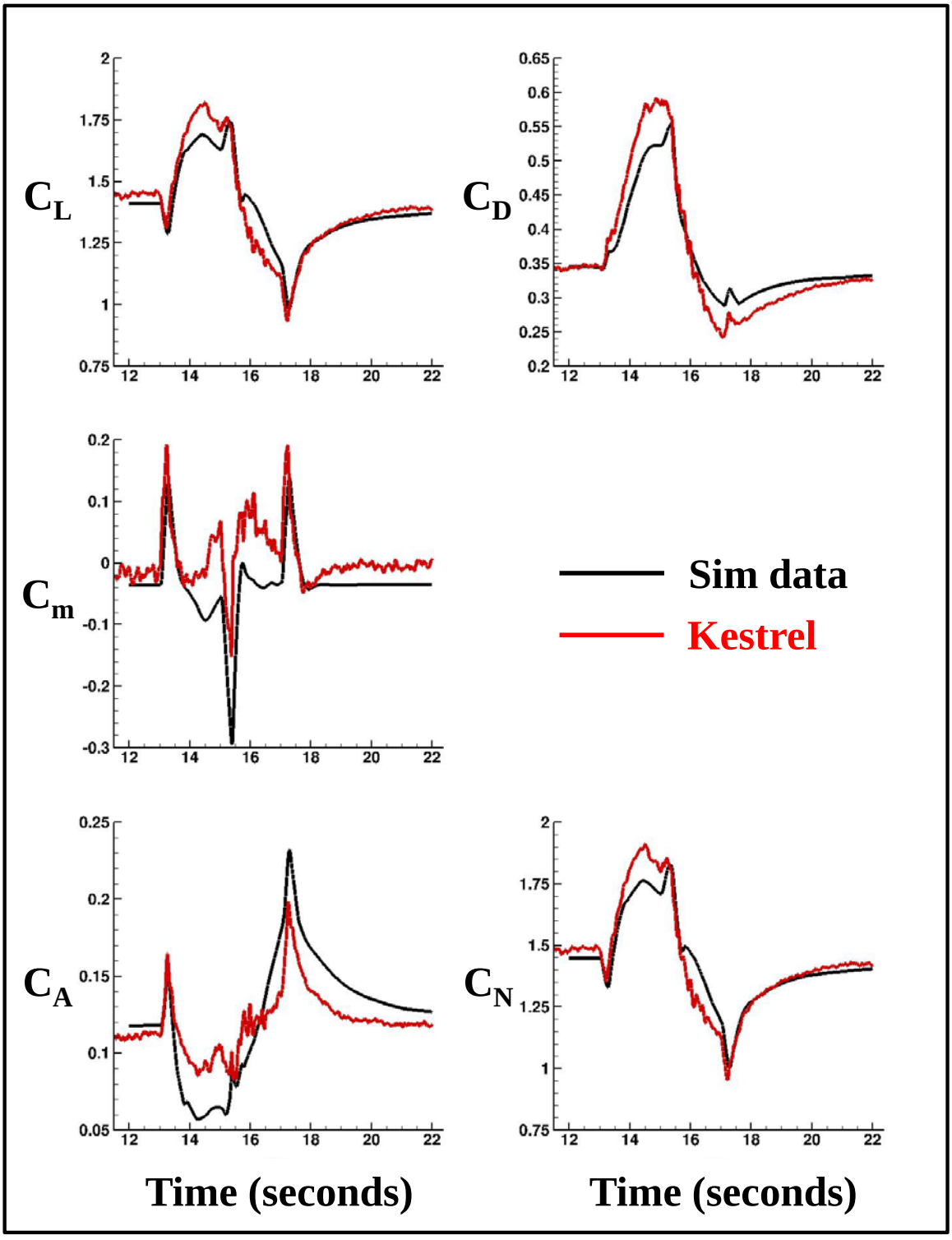

Figure 29: Longitudinal Force and Moment Coefficients for Kestrel and Sim Data for the F/A-18E Trimmed Longitudinal Stick Doublet Maneuver at Mach 0.2 and an Altitude of 1,240 ft

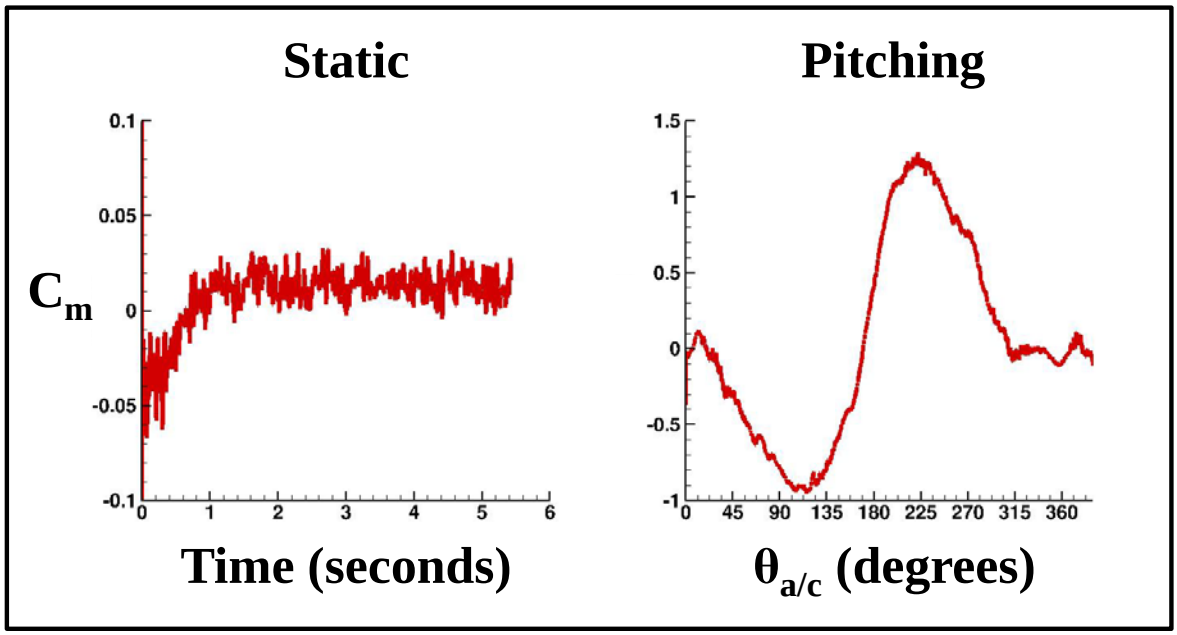

Figure 30: Pitching-Moment Coefficients for the Static and Pitching F/A-18E for the Pitch-Damping Calculations

THIS PAGE INTENTIONALLY LEFT BLANK

DISTRIBUTION:

NAVAIRSYSCOM (AIR-4.3.2), david.findlay@navy.mil
NAVAIRSYSCOM (AIR-4.3.2.1), bradford.green@navy.mil
NAVAIRSYSCOM (AIR-4.3.2.1), frank.taverna@navy.mil
NAVAIRSYSCOM (AIR-4.3.2), steven.donaldson@navy.mil
NAVAIRSYSCOM (AIR-4.3.2.1), joseph.laiosa@navy.mil
ONR 35, Thomas.beutner@navy.mil, knox.millsaps@navy.mil
ONR 351, Kenneth.iwanski@navy.mil; brian.holm-hansen@navy.mil
ONR 352, Kenneth.heeke@navy.mil